Day 3

Part 2: From imaging to inversion

1942

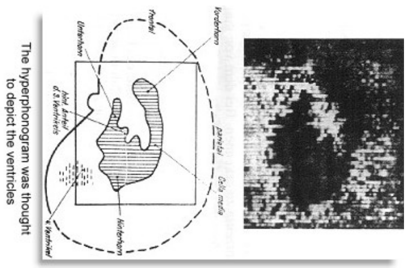

2020

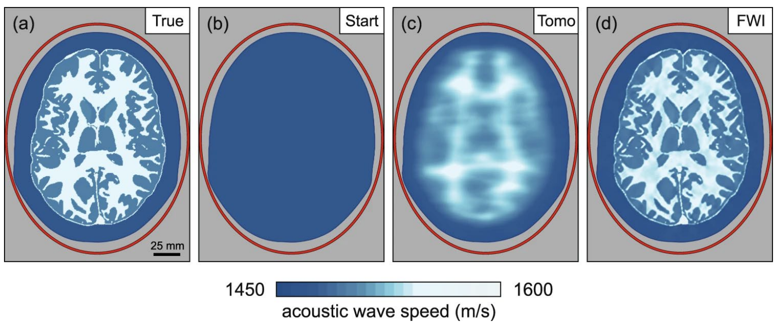

Dussik, https://www.ob-ultrasound.net/dussikbio.html
Guasch, *et al.* Full-waveform inversion imaging of the human brain. *npj Digit. Med.* **3**, 28 (2020)

Delft University of Technology

Conventional Ultrasound Imaging

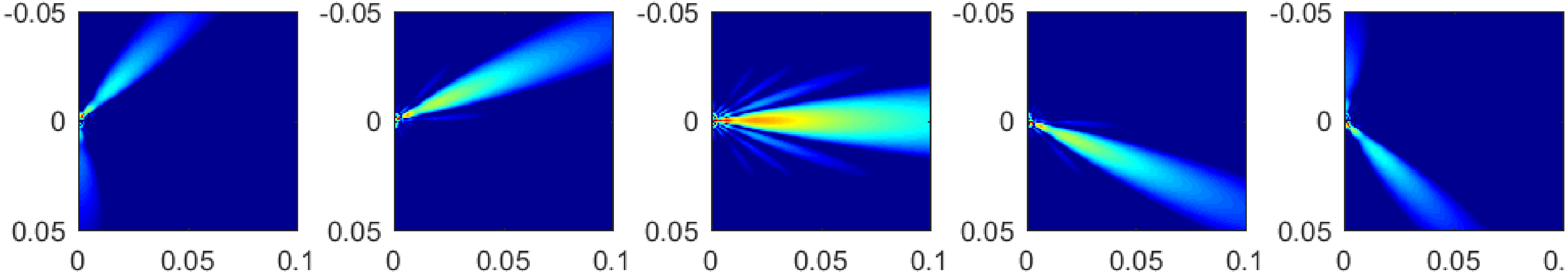

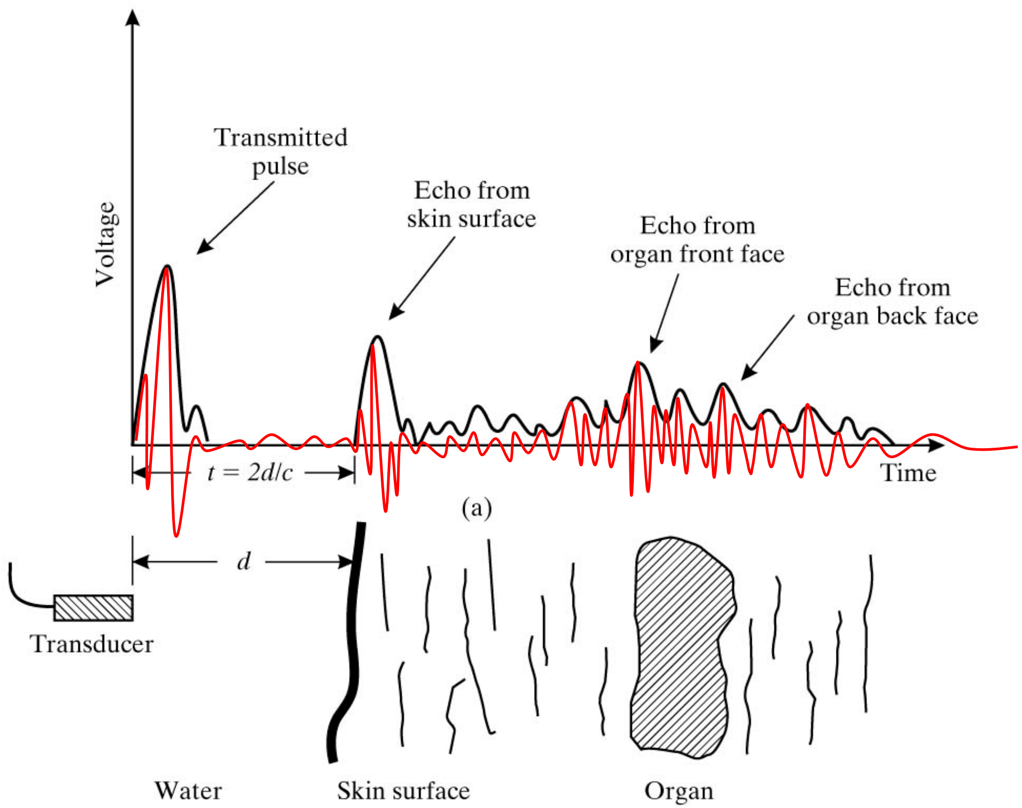

Heterogeneous Media

- Incident, scattered and total field
- Forward and inverse problem

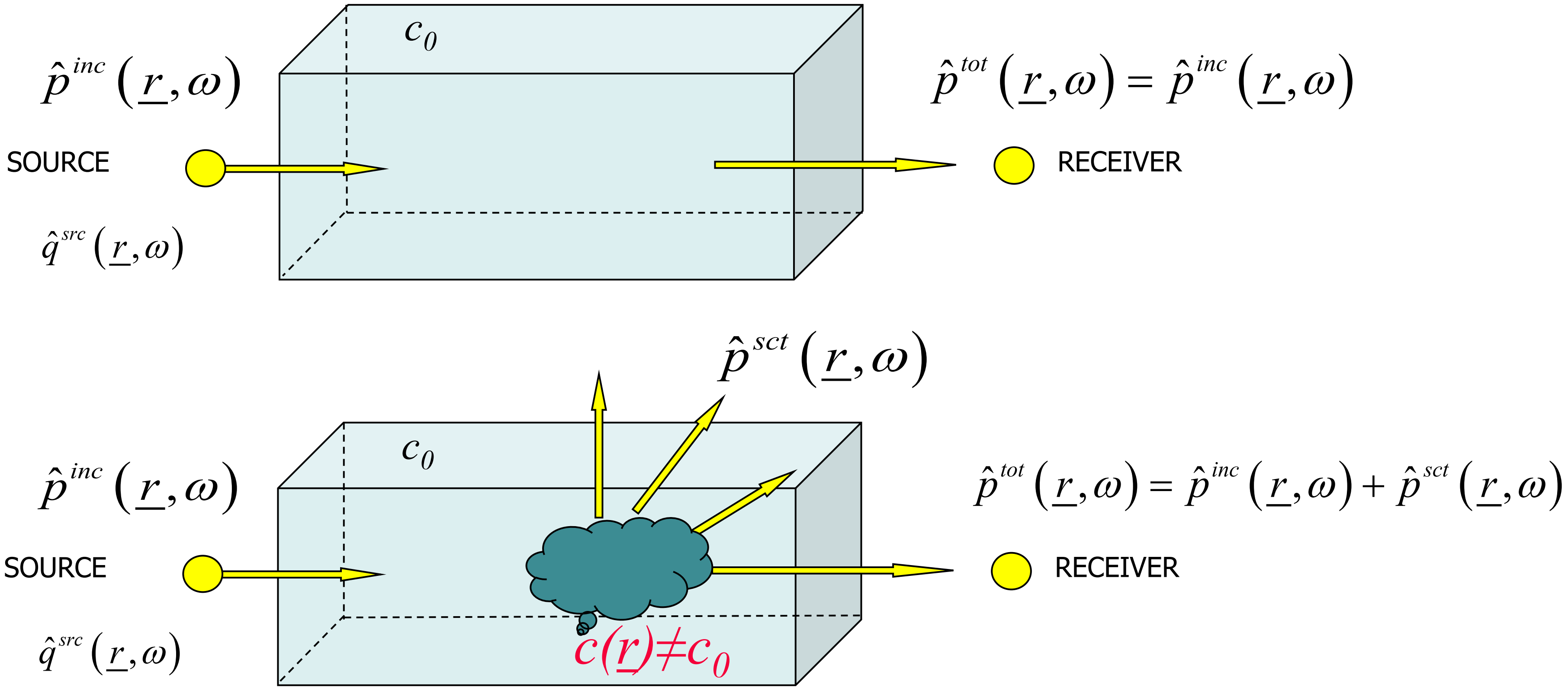

Acoustic wave equation

Wave equation:

$$\nabla^2 p(\vec{x},t) - \frac{1}{c^2(\vec{x})}\partial_t^2 p(\vec{x},t) = -S^{pr}(\vec{x},t)$$

Helmholtz equation:

$$\nabla^2 p(\vec{x}) + \frac{\omega^2}{c_{bg}^2} p(\vec{x}) = -S^{pr}(\vec{x}) + \omega^2 \underbrace{\left(\frac{1}{c_{bg}^2} - \frac{1}{c^2(\vec{x})}\right)}_{=\chi(\vec{x})} p(\vec{x})$$

Integral equation:

$$p(\vec{x}) = p^{inc}(\vec{x}) - \omega^2 \int G(\vec{x}-\vec{x}\,')\,\chi(\vec{x}\,')\,p(\vec{x}\,')\,\mathrm{d}V(\vec{x}\,')$$

with $G(\vec{x}) = \dfrac{e^{-ik|\vec{x}|}}{4\pi|\vec{x}|}$

$$p^{inc} = p + G[p] \quad \rightarrow \quad b = A[x]$$

$$r_n = b - A[x_n]$$

$$x_n = x_{n-1} + \alpha d_n$$

$$d_n = A^{\dagger}[r_n]$$

Breast ultrasound

- Leading cause of death for women (in Western World)
- Screening with mammography is

  painful, expensive, risks (radiation), limited to elderly women

Alternative: ultrasound?

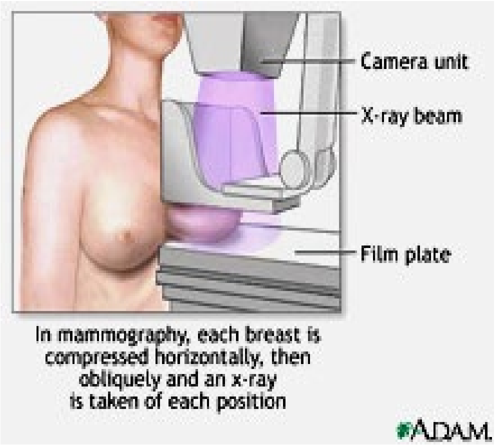

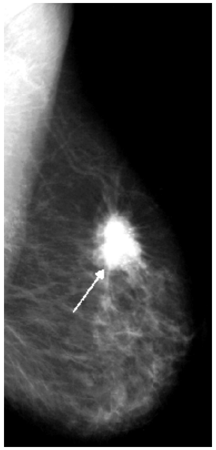

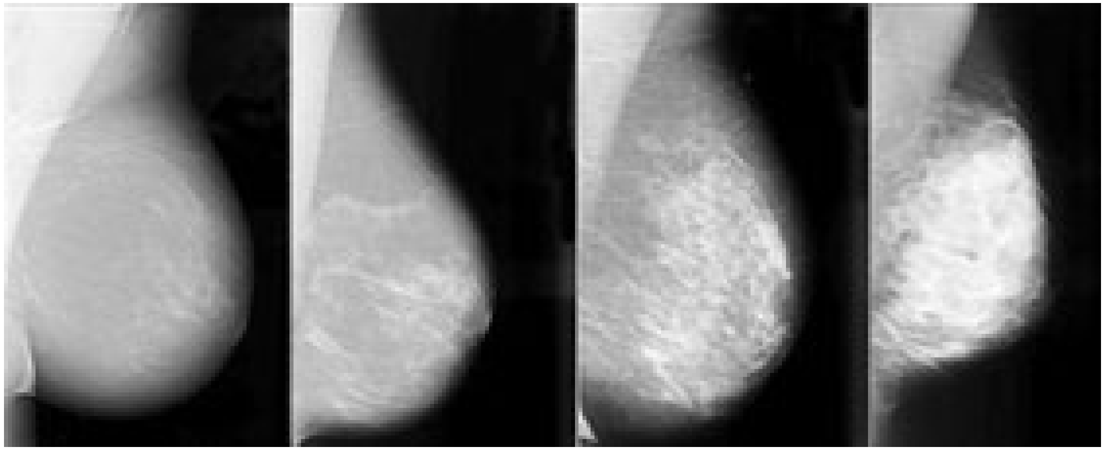

Breast ultrasound – Siemens Acuson

siemens.com

TU Delft / Erasmus MC Netherlands

Reflectivity versus quantitative imaging

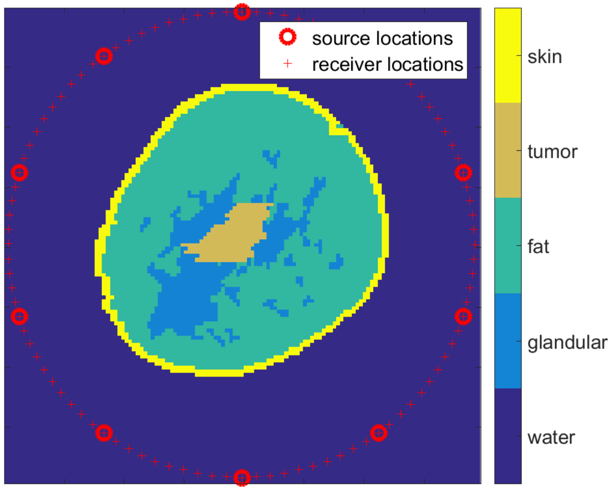

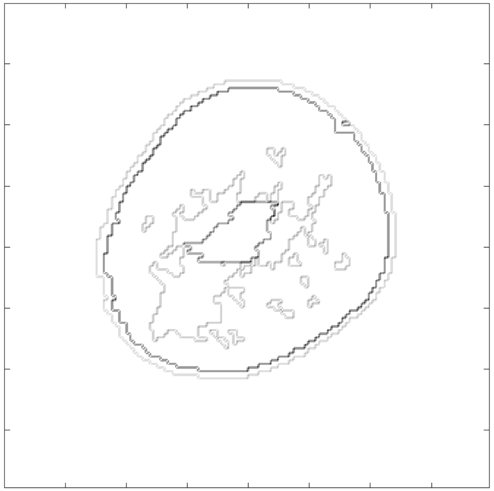

$$R = \frac{c_2 - c_1}{c_2 + c_1}$$

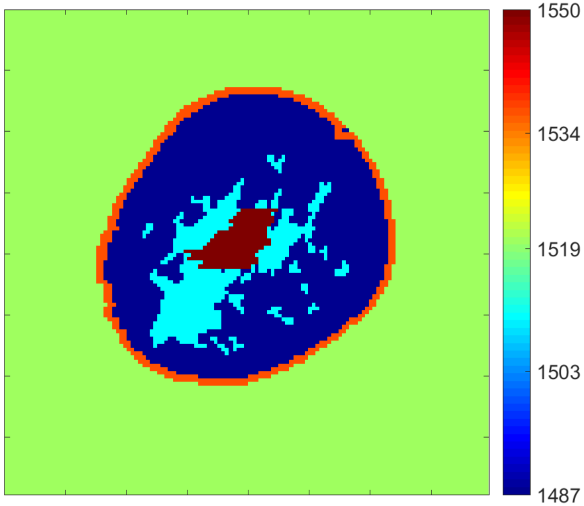

Speed of sound
Density
Compressibility
Absorption

Tissue characterisation

TU Delft

Breast ultrasound - an (old) overview

SomoVu	ACUSON	USCT	Wrocław Univ. of Technology	SoftVue	Techniscan - QT Imaging
f_0 = 9 MHz (λ_0 = 0.2 mm)	8 MHz (0.2 mm)	2.5 MHz (0.6 mm)	2 MHz (0.75 mm)	3 MHz (0.5 mm)	1.6 & 5 MHz (0.9 - 0.3 mm)



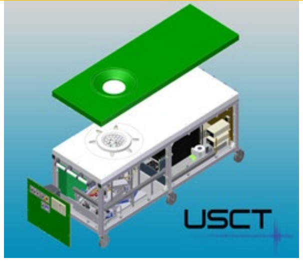


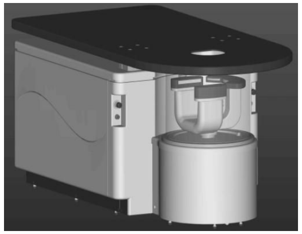


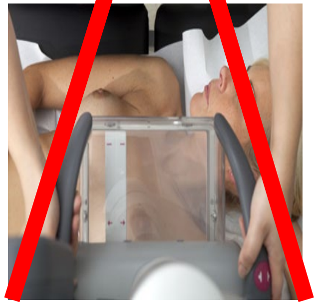

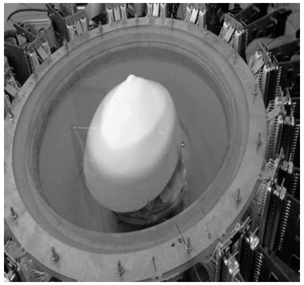

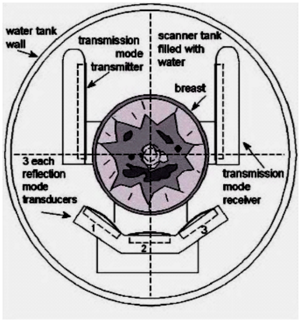

TU Delft

Heterogeneous media – field equations

Hooke's law: $\nabla \cdot \underline{v}(\underline{r},t) + \kappa(\underline{r}) \partial_t p(\underline{r},t) = q(\underline{r},t) \quad \Rightarrow$

$$\nabla \cdot \underline{v}(\underline{r},t) + \kappa_0 \partial_t p(\underline{r},t) = q(\underline{r},t) + \{\kappa_0 - \kappa(\underline{r})\} \partial_t p(\underline{r},t)$$

Newton's law: $\nabla p(\underline{r},t) + \rho(\underline{r}) \partial_t \underline{v}(\underline{r},t) = \underline{f}(\underline{r},t) \quad \Rightarrow$

$$\nabla p(\underline{r},t) + \rho_0 \partial_t \underline{v}(\underline{r},t) = \underline{f}(\underline{r},t) + \{\rho_0 - \rho(\underline{r})\} \partial_t \underline{v}(\underline{r},t)$$

Combining the above field equations yields the wave equation

$$\nabla^2 p(\underline{r},t) - \frac{1}{c_0^2} \partial_t^2 p(\underline{r},t) = -\underbrace{\{\rho_0 \partial_t q(\underline{r},t) - \nabla \cdot \underline{f}(\underline{r},t)\}}_{S_{pr}(\underline{r},t)}$$

$$-\underbrace{\{\rho_0 (\kappa_0 - \kappa(\underline{r})) \partial_t^2 p(\underline{r},t) - \nabla \cdot [\{\rho_0 - \rho(\underline{r})\} \partial_t \underline{v}(\underline{r},t)]\}}_{S_{cs}(\underline{r},t)}$$

attenuation

$$\frac{1}{c^2(\underline{r})} = \rho_0 \kappa(\underline{r})$$

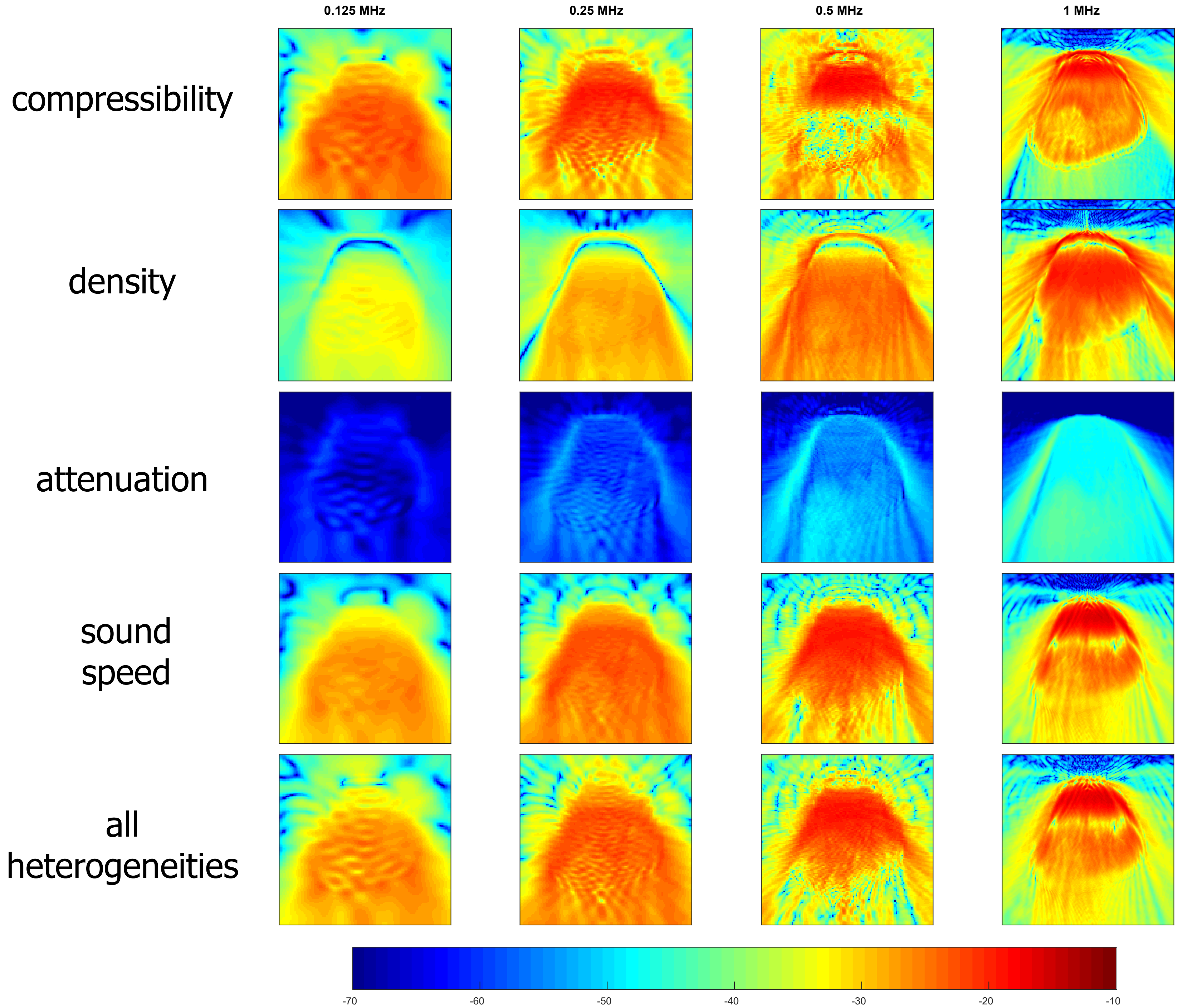

0.125 MHz
0.25 MHz
0.5 MHz
1 MHz
compressibility
density
attenuation
sound speed
all heterogeneities
-70
-60
-50
-40
-30
-20
-10

Forward versus Inverse Problem

- Incident, scattered and total field

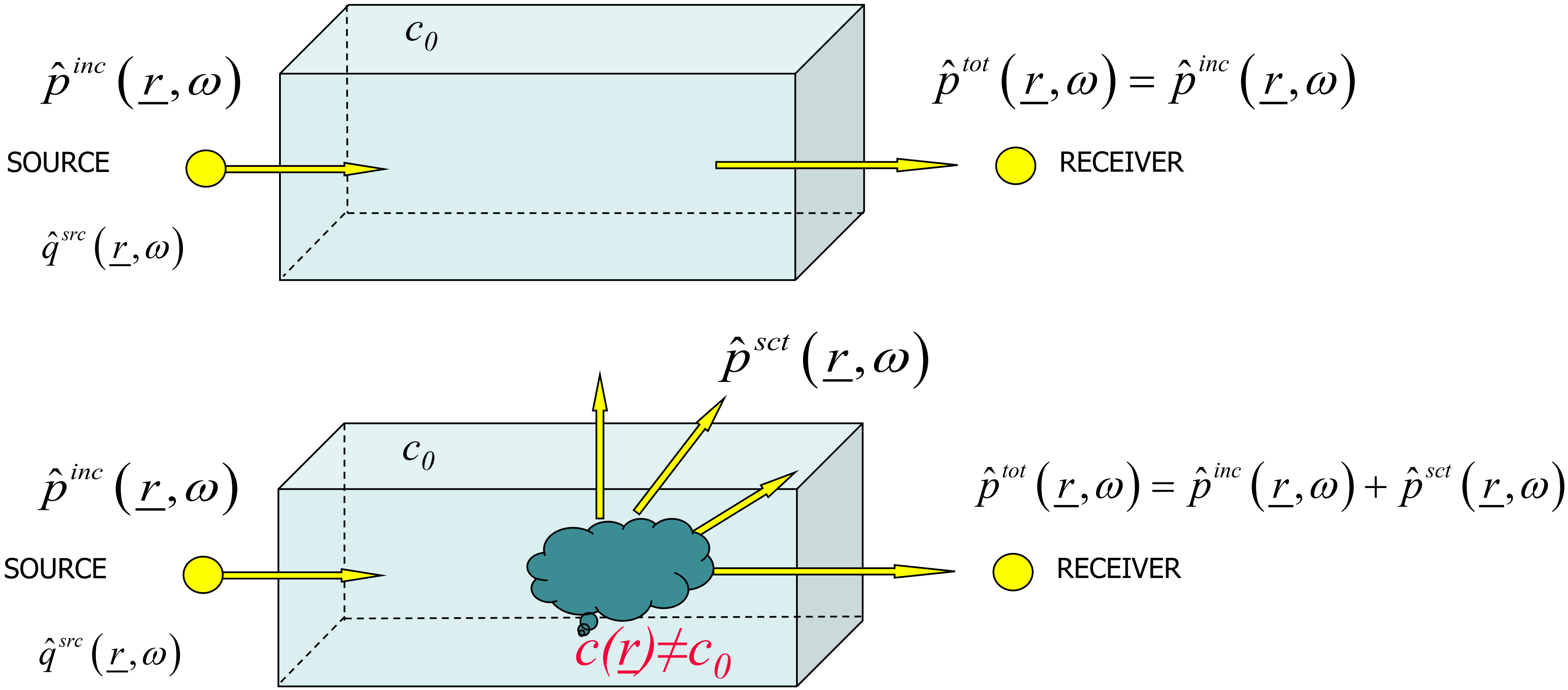

Acoustic wave equation – forward problem

Wave equation: $$\nabla^2 p(\vec{x},t) - \frac{1}{c^2(\vec{x})}\partial_t^2 p(\vec{x},t) = -S^{pr}(\vec{x},t)$$

Helmholtz equation: $$\nabla^2 p(\vec{x}) + \frac{\omega^2}{c_{bg}^2} p(\vec{x}) = -S^{pr}(\vec{x}) + \omega^2 \underbrace{\left(\frac{1}{c_{bg}^2} - \frac{1}{c^2(\vec{x})}\right)}_{=\chi(\vec{x})} p(\vec{x})$$

Radon transform: $$\Delta t_\beta(\gamma) = \int \frac{1}{c(\vec{x})}\, \mathrm{d}\vec{s}(\vec{x})$$

Parabolic approximation:

$$p(k_x, k_y, z_0 + \Delta) = p(k_x, k_y, z_0)\, e^{-ik_z\Delta}$$ with $$k_z = k_{mean} + (k_x^2 + k_y^2) / 2k_{mean}$$

Integral equation:

Born approx.: $p \rightarrow p^{inc}$

$$p(\vec{x}) = p^{inc}(\vec{x}) - \omega^2 \int G(\vec{x} - \vec{x}')\, \chi(\vec{x}')\, p(\vec{x}')\, \mathrm{d}V(\vec{x}')$$ with $$G(\vec{x}) = \frac{e^{-ik|\vec{x}|}}{4\pi |\vec{x}|}$$

Breast Ultrasound

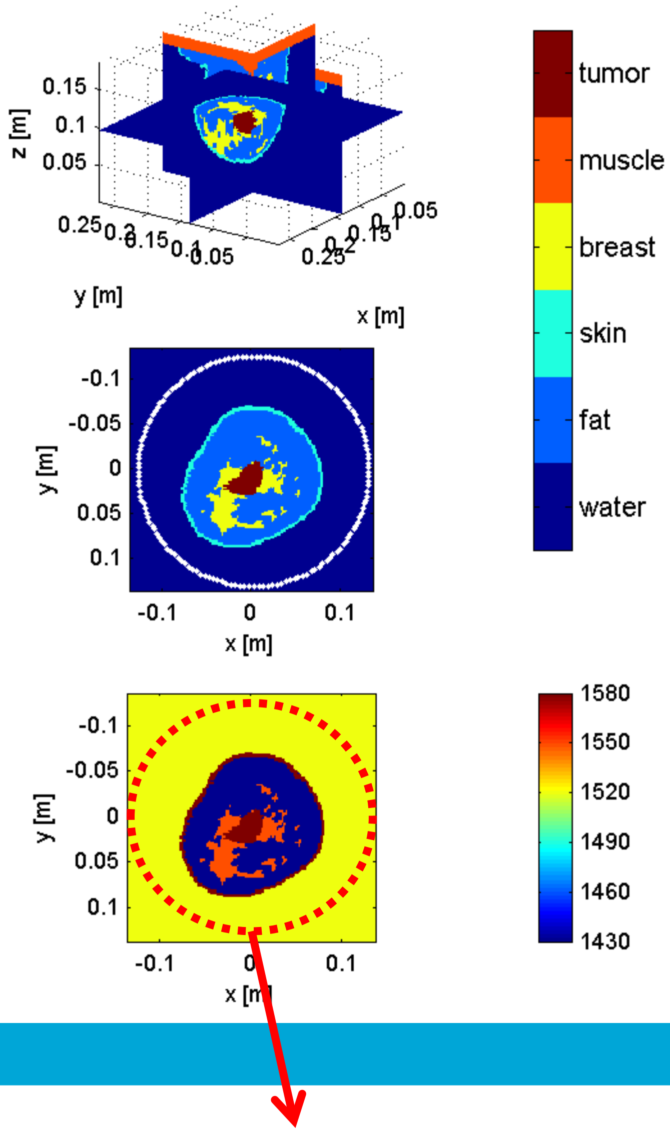

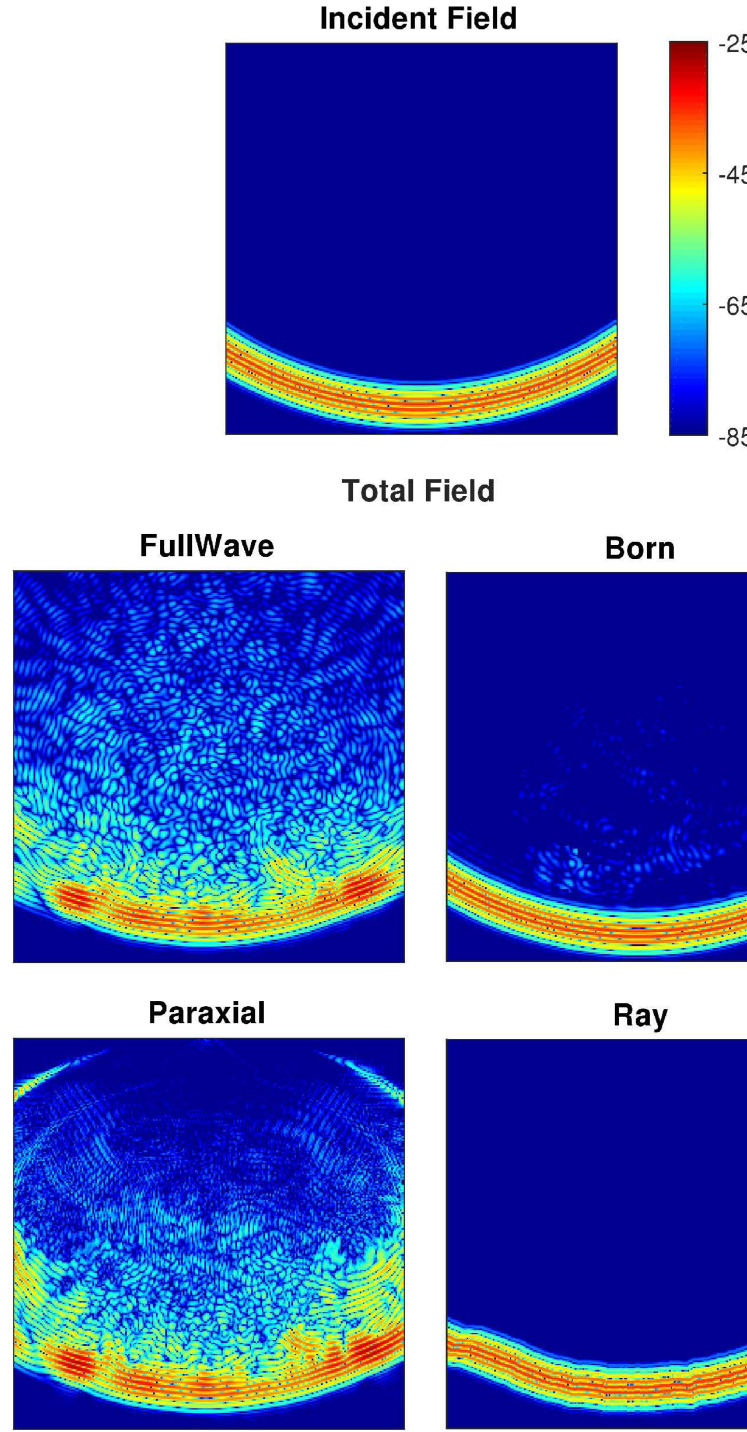

Ring with transducers

Breast ultrasound

Synthetic data obtained by solving forward problem for each source.

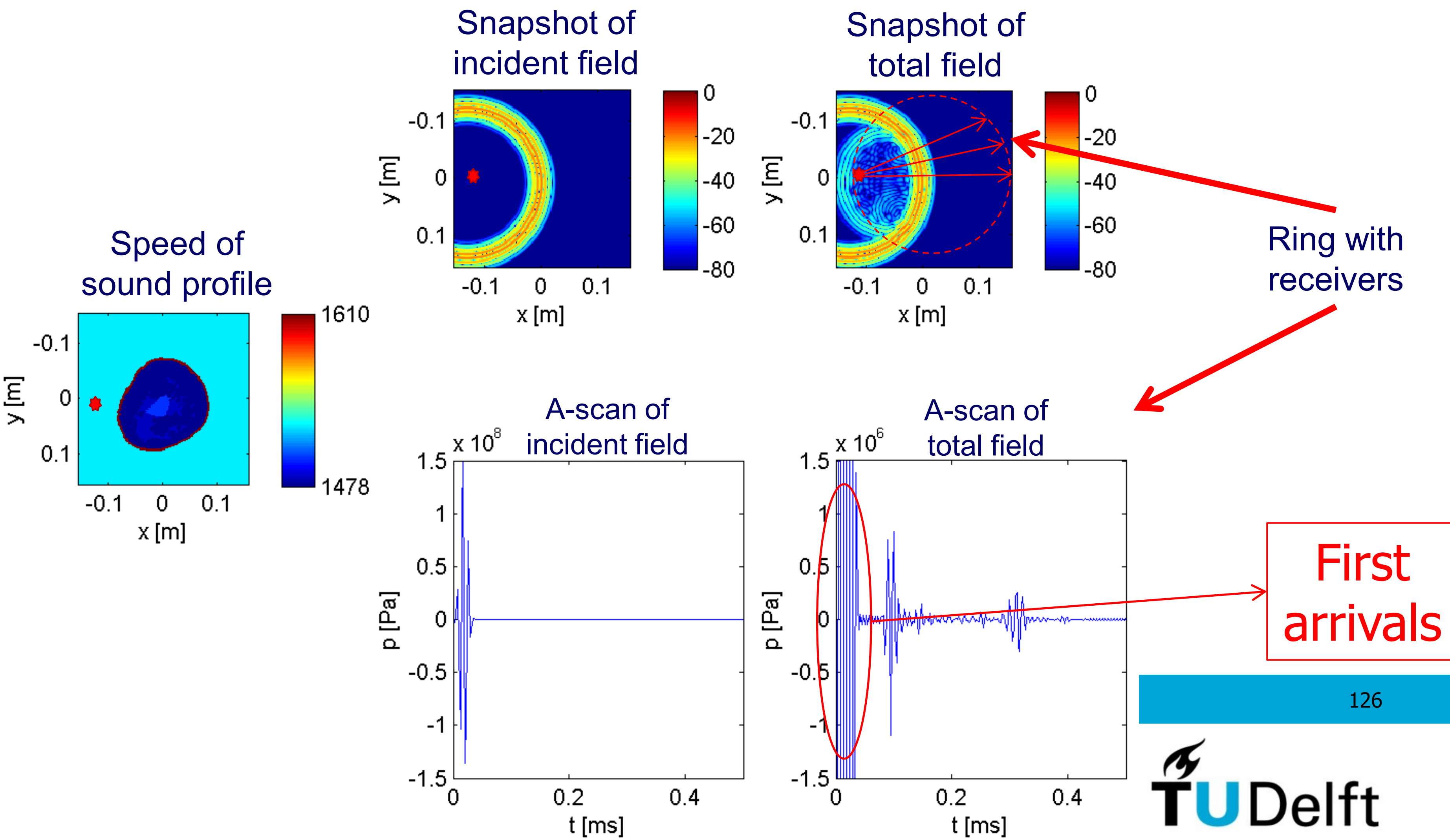

TU Delft

Inverse radon

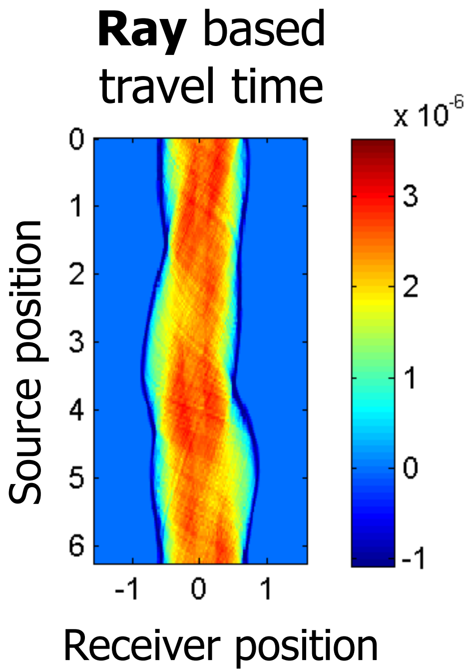

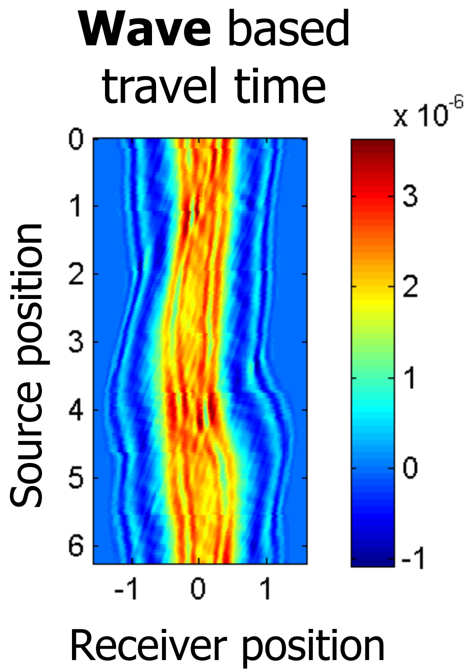

Inverse radon

- Bezier Curves: $B(t)=(1-t)^2P_0+2t(1-t)P_1+t^2P_2$
- MUBI system
  - >3MHz
  - $N_{Src/Rec}$ = N x 128

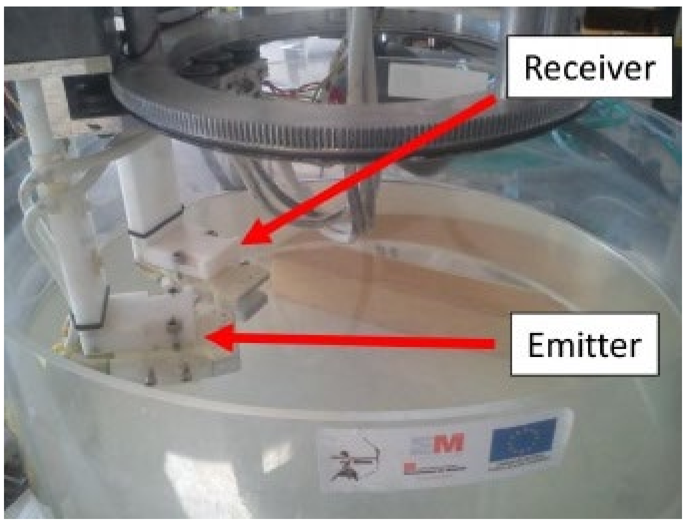

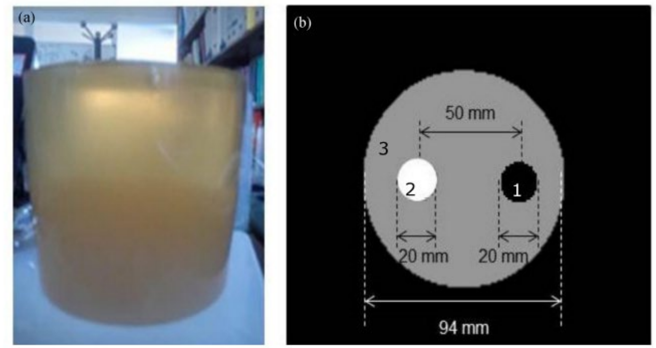

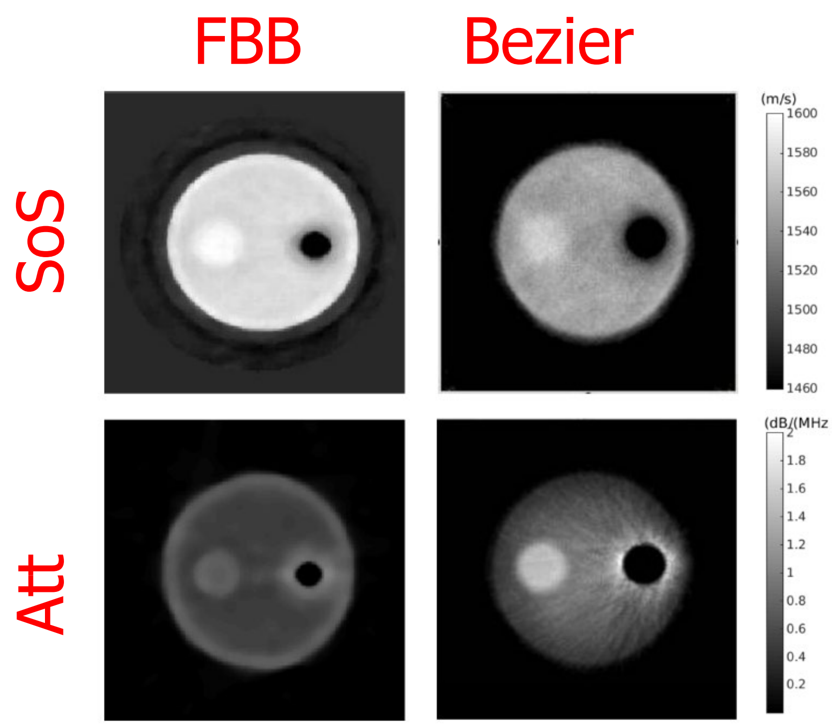

M. Perez-Liva, et al, "Real-Time Ultrasound Transmission Tomography based on Bézier Curves", Speyer 2017

Parabolic approximation (QT Ultrasound)

- $$p(k_x, k_y, z_0 + \Delta) = p(k_x, k_y, z_0)\, e^{-ik_z\Delta}$$
- Solution based on CG
- Out of plane scattering
- 3D formulation (with parts in 2D?)

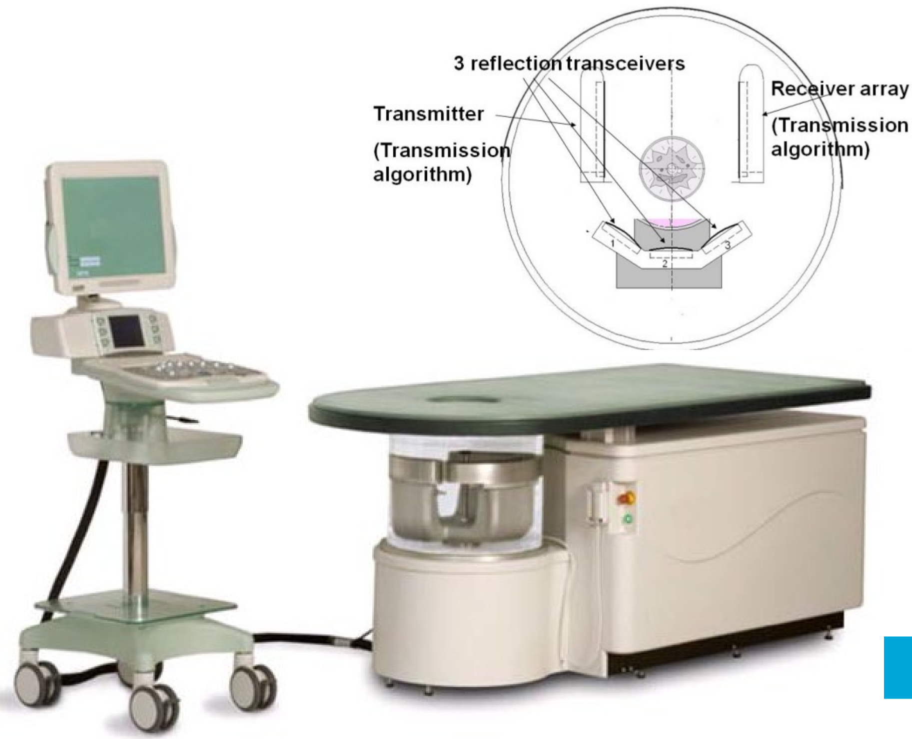

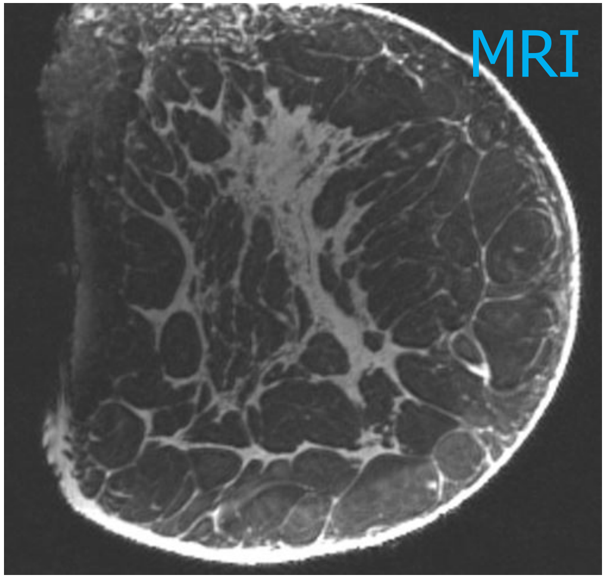

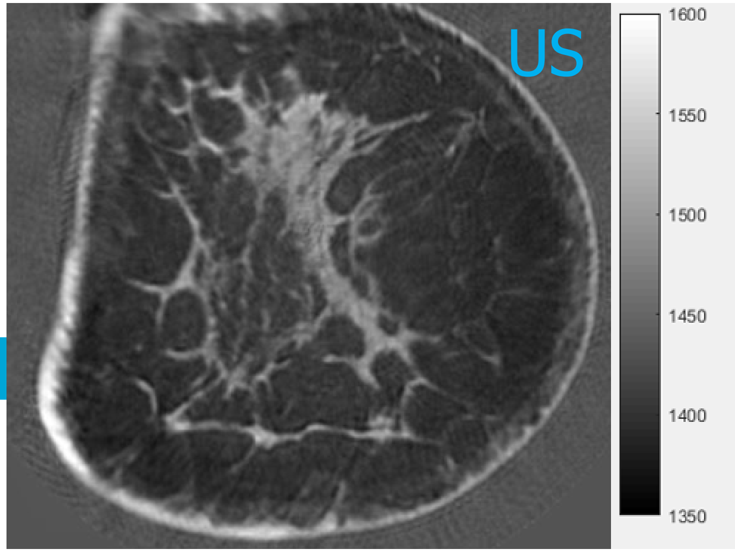

Wiskin et al. "3-D Nonlinear Acoustic Inverse Scattering: Algorithm and Quantitative Results", IEEE Trans. UFFC 2017.

Breast ultrasound

Synthetic data obtained by solving forward problem for each source.

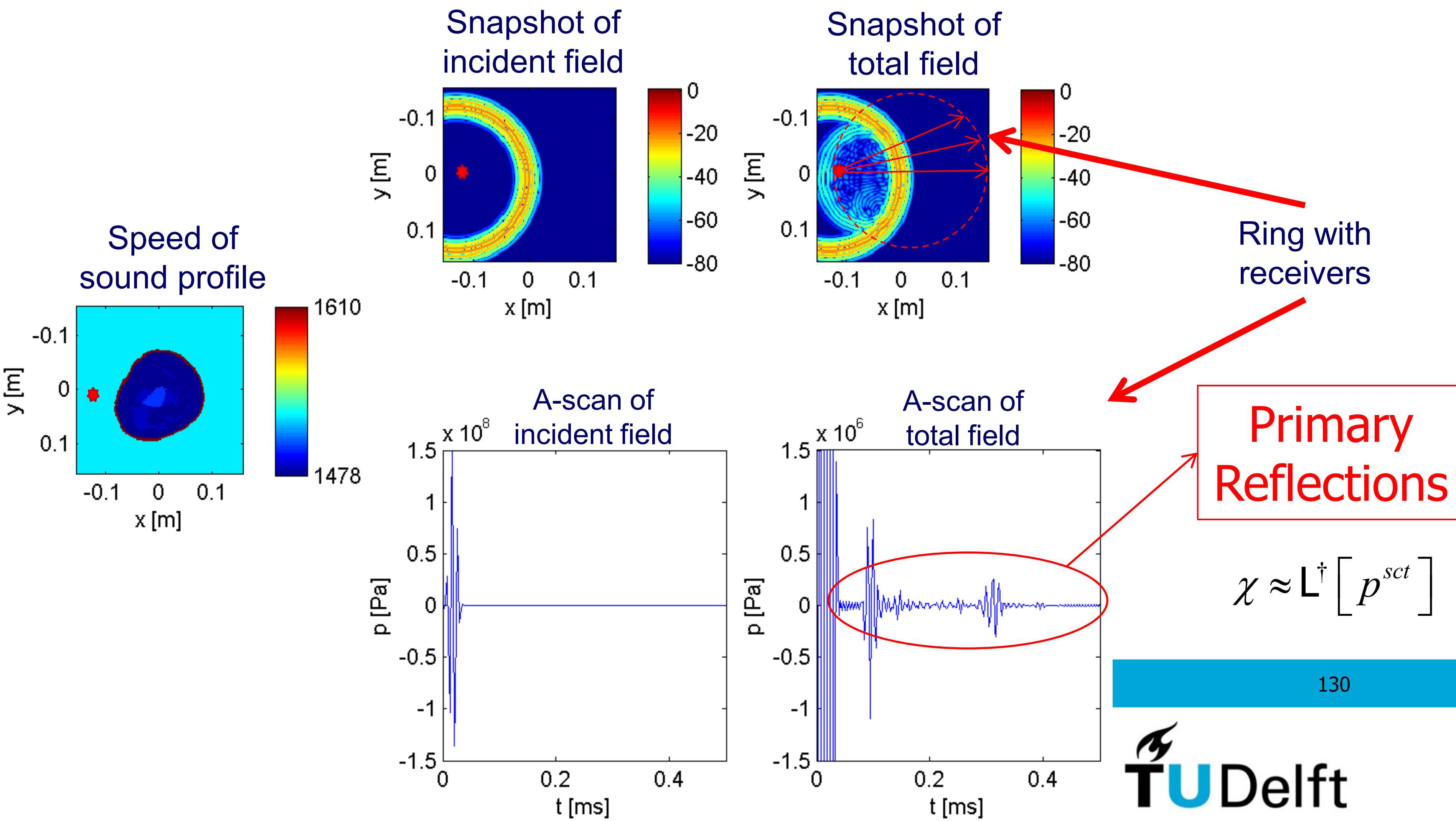

$$\chi \approx \mathsf{L}^{\dagger}\left[p^{sct} \right]$$

Imaging: SAFT / SAR / DAS

Synthetic Aperture Focusing Technique
Synthetic Aperture Radar
Delay and Sum

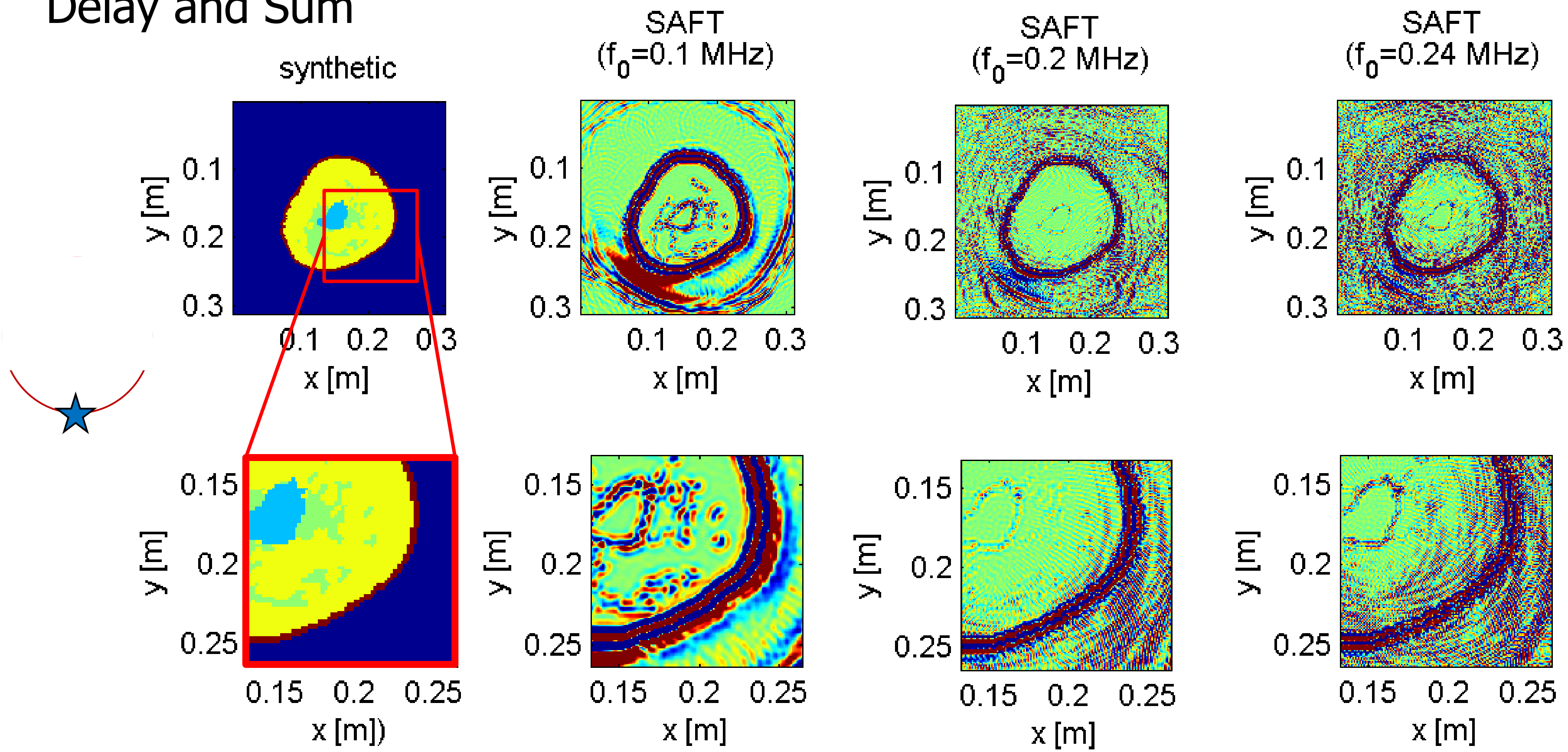

TU Delft

SAFT

SoS

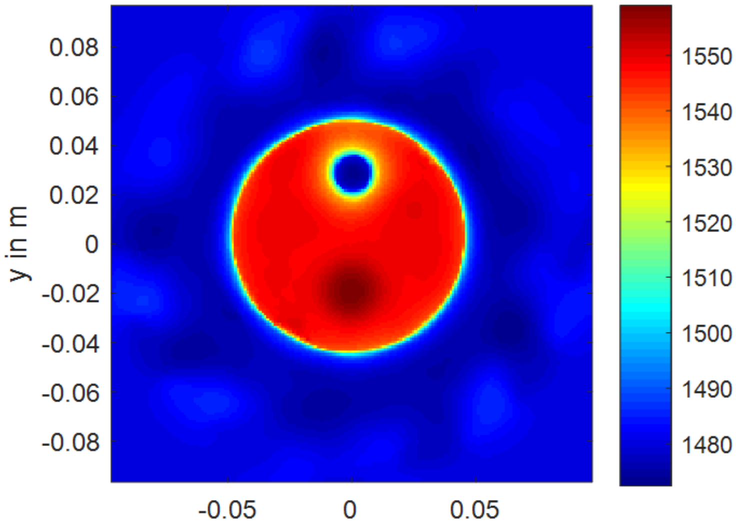

Attenuation

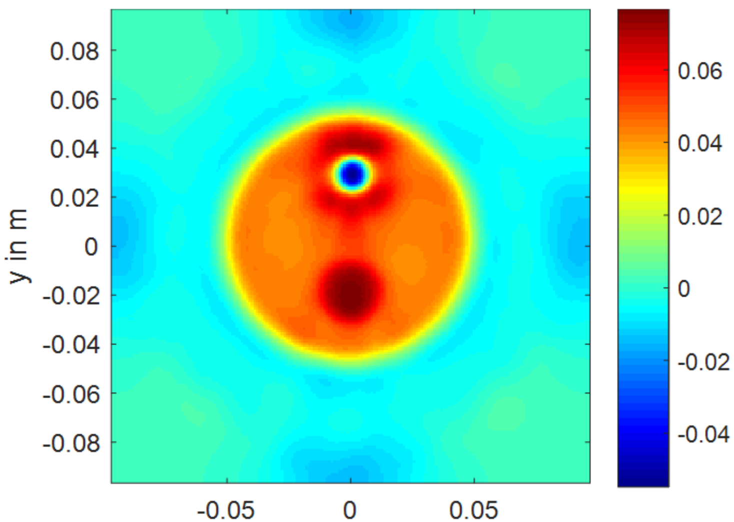

Saft (MUBI-system)

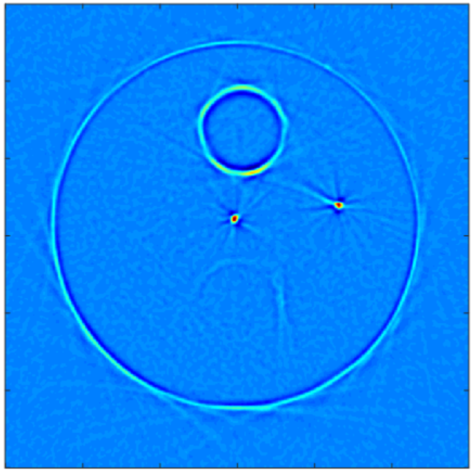

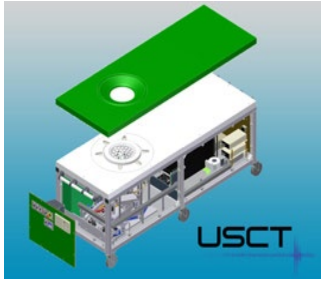

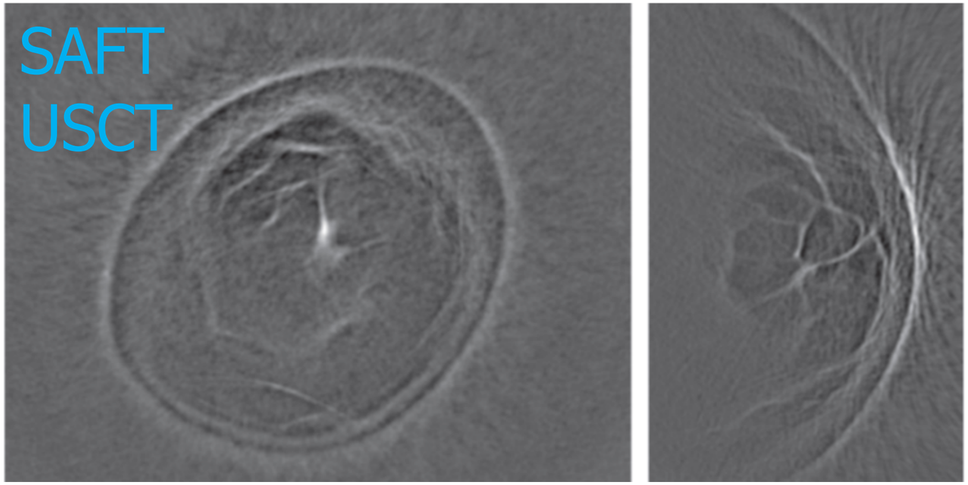

N.V. Ruiter, et. al. "The USCT reference database", Speyer (2017)
N.V. Ruiter, et. al. "Fast reflectivity imaging in 3D using SAFT", Speyer (2017)

TU Delft

Acoustic wave equation based inversion

Wave equation:

$$\nabla^2 p(\vec{x},t) - \frac{1}{c^2(\vec{x})}\partial_t^2 p(\vec{x},t) = -S^{pr}(\vec{x},t)$$

Helmholtz equation:

$$\nabla^2 p(\vec{x}) + \frac{\omega^2}{c_{bg}^2} p(\vec{x}) = -S^{pr}(\vec{x}) + \omega^2 \underbrace{\left(\frac{1}{c_{bg}^2} - \frac{1}{c^2(\vec{x})}\right)}_{=\chi(\vec{x})} p(\vec{x})$$

TUDelft

Inverse problem – Born inversion (linearized inversion)

$$p(\vec{x}) = p^{inc}(\vec{x}) - \omega^2 \int G(\vec{x}-\vec{x}')\, \boxed{\chi(\vec{x}')\; p(\vec{x}')}\, \mathrm{d}V(\vec{x}')$$

Born Approximation:

$$p(\vec{x}) = p^{inc}(\vec{x}) - \omega^2 \int G(\vec{x}-\vec{x}')\; \chi(\vec{x}')\; p^{inc}(\vec{x}')\, \mathrm{d}V(\vec{x}')$$

$$p - p^{inc} = -\omega^2 G * [\chi\, p^{inc}]$$

(b=Ax) Conjuge gradient scheme

$$r_n = p^{sct} - \omega^2 G * [\chi_n p^{inc}]$$

$$\chi_n = \chi_{n-1} + d_n$$

Linear or Born Inversion

Linear Inversion is an unstable process due to the Born-approximation.

$n_{it} = 512$

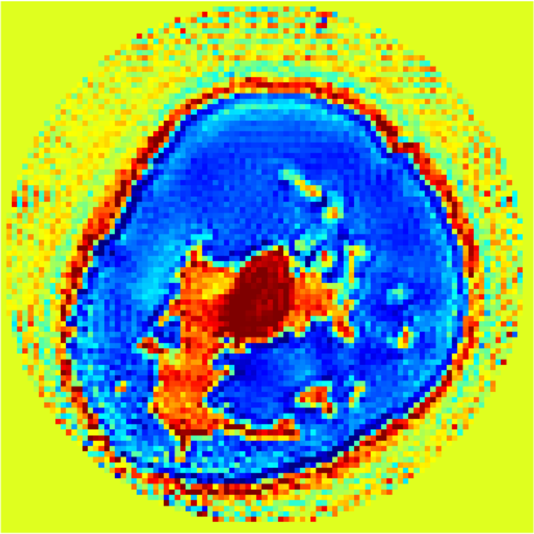

Breast ultrasound

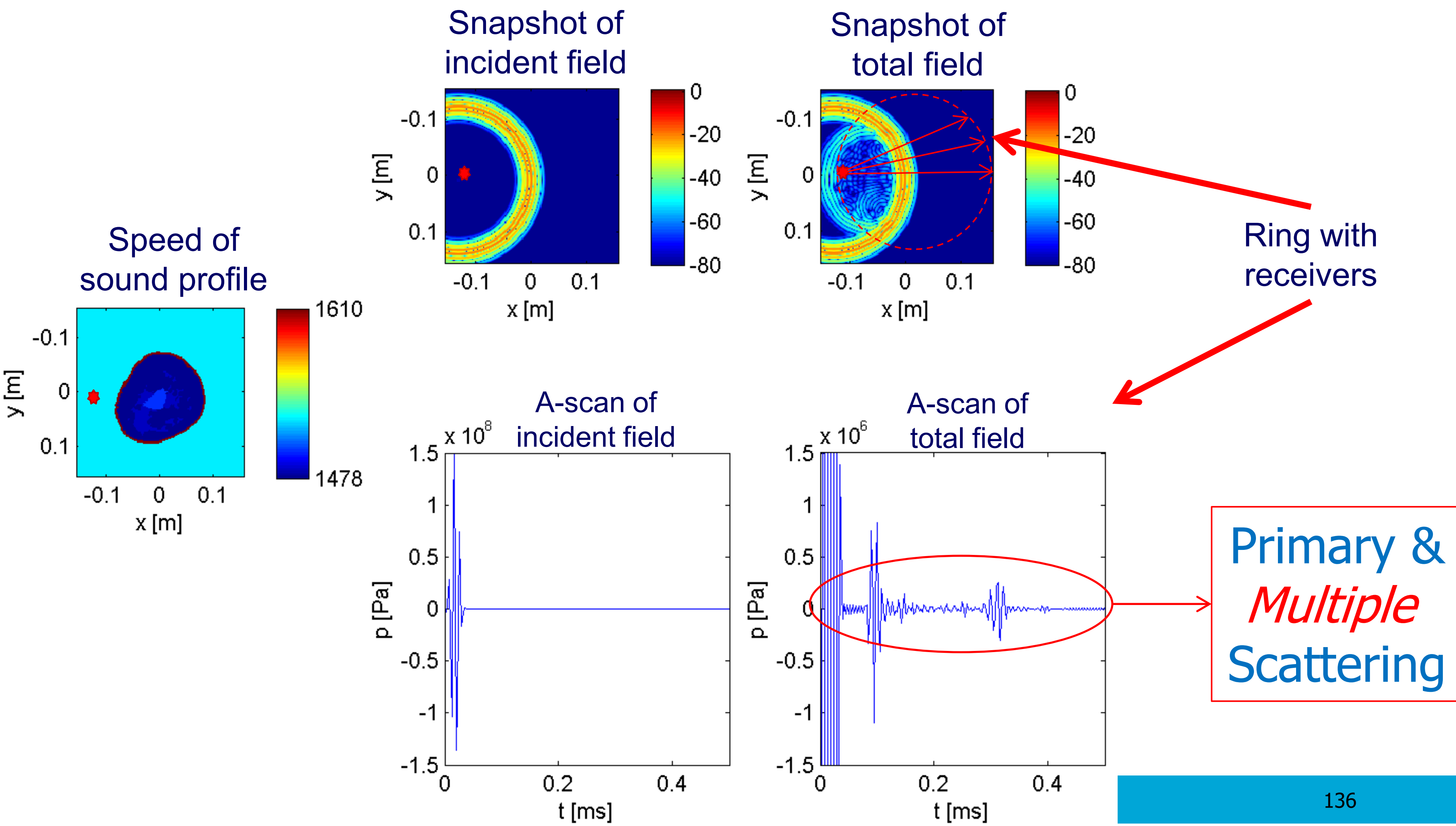

TU Delft

Wave equation

- $$\nabla^2 p(\vec{x},t) - \frac{1}{c^2(\vec{x})}\partial_t^2 p(\vec{x},t) = -S^{pr}(\vec{x},t$$
- 2-D inversion

  (3D too expensive)

- CURE system

  (Karmanos Cancer Institute)

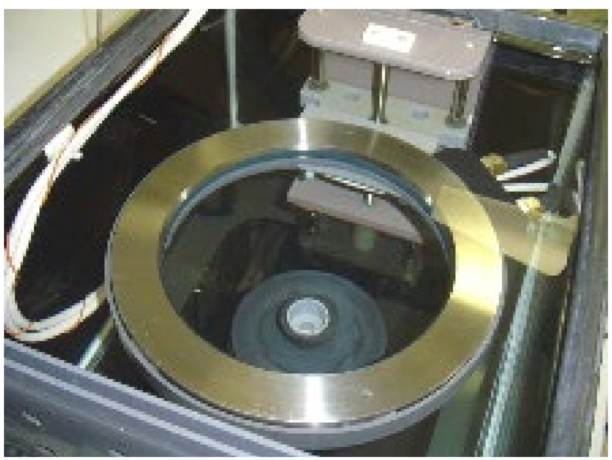

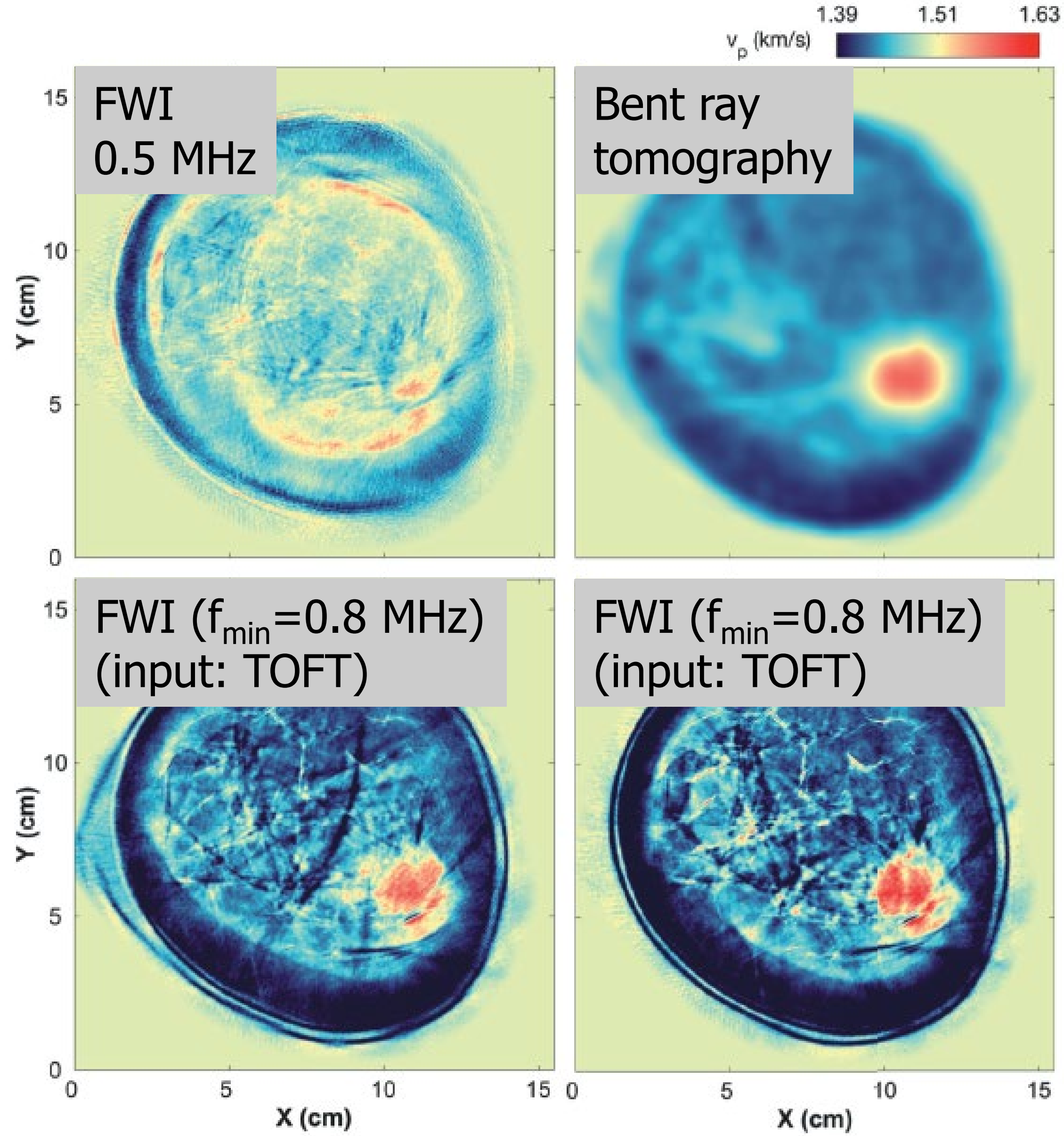

Figure 7: Recovered models of speed of sound obtained from the 2D *in vivo* data after using a) FWI at $f_{min} = 500kHz$ and a constant water starting model, b) bent-ray tomography and FWI with the time-of-flight model as a starting model at c) $f_{min} = 800kHz$ and d) at $f_{min} = 500kHz$. The maximum frequency for all FWI tests is $1.75MHz$.

Agudo, et al, "3D imaging of the breast using FWI", Speyer (2017)

Inverse problem – non-linear inversion
(full-waveform inversion – FWI – contrast source inversion – CSI)

$$p(\vec{x}) = p^{inc}(\vec{x}) - \omega^2 \int G(\vec{x}-\vec{x}')\, \chi(\vec{x}')\, p(\vec{x}')\, \mathrm{d}V(\vec{x}')$$

Born Approximation:

$$p(\vec{x}) = p^{inc}(\vec{x}) - \omega^2 \int G(\vec{x}-\vec{x}')\, \chi(\vec{x}')\, p^{inc}(\vec{x}')\, \mathrm{d}V(\vec{x}')$$

Full non-linear inversion:

$$p(\vec{x}) = p^{inc}(\vec{x}) - \omega^2 \int G(\vec{x}-\vec{x}')\, w(\vec{x}')\, \mathrm{d}V(\vec{x}') \qquad p^{tot} = p^{inc} - \omega^2 G * w$$

$$w(\vec{x}') = \chi(\vec{x}')\, p(\vec{x}') \qquad w = \chi\, p^{tot}$$

$$Err_n = \frac{\left\| p - \left(p^{inc} - \omega^2 G * w_n \right) \right\|^2}{\left\| p^{inc} \right\|^2} + \frac{\left\| w_n - \chi_{n-1} \left(p^{inc} - \omega^2 G * w_n \right) \right\|^2}{\left\| \chi_{n-1} p^{inc} \right\|^2}$$

TU Delft

Non-Linear Inversion

- Non-linear Inversion is a stable process as it uses the full wave equation.

$n_{it} = 1024$

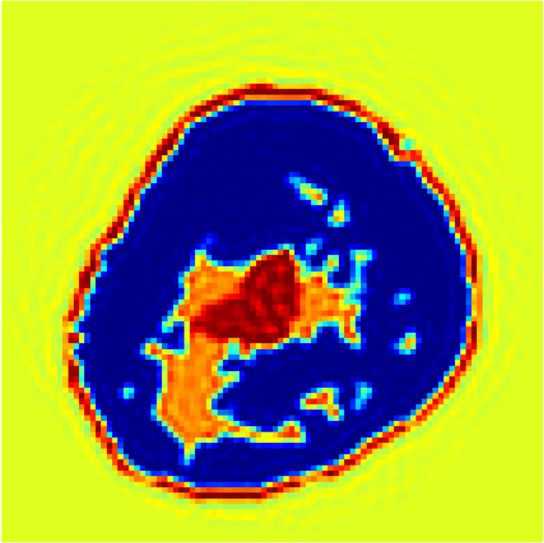

Non-linear inversion

$$p^{tot}(\vec{r}) = p^{inc}(\vec{r}) - \int G(\vec{r}-\vec{r}\,')\,\omega^2 \chi(\vec{r}\,')\, p^{tot}(\vec{r}\,')\,\mathrm{d}V$$

Born Approximation:

$$\hat{p}^{tot}(\vec{r}) = \hat{p}^{inc}(\vec{r}) - \omega^2 \int \hat{G}(\vec{r}-\vec{r}\,')\,\chi(\vec{r}\,')\,\hat{p}^{inc}(\vec{r}\,')\,\mathrm{d}V$$

Full non-linear inversion:

$$\hat{p}^{tot}(\vec{r}) = \hat{p}^{inc}(\vec{r}) - \omega^2 \int \hat{G}(\vec{r}-\vec{r}\,')\,\hat{w}(\vec{r}\,')\,\mathrm{d}V$$

$$\hat{w}(\vec{r}\,') = \chi(\vec{r}\,')\hat{p}^{tot}(\vec{r}\,')$$

$$p^{tot} = p^{inc} - G * w$$

$$w = \chi p^{tot}$$

Regularization

- Total Variation
- sparsity
  - w
  - χ

$$Err^{(n)} = \left[\frac{\left\|p^{tot} - p^{inc} + G * w^{(n)}\right\|}{\left\|p^{inc}\right\|} + \frac{\left\|w^{(n)} - \chi^{(n-1)}\left(p^{inc} - G * w^{(n)}\right)\right\|}{\left\|\chi^{(n-1)} p^{inc}\right\|}\right] + (\ldots)$$

TUDelft

5% noise

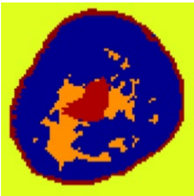

$$E_{TV} = \eta_{TV} \int_{\vec{x}\in D} \sqrt{\left|\nabla \chi_n(\vec{x})\right|^2}\, dA$$

$$\eta_S E_S + \eta_D E_D$$

$$s.t. \begin{cases} \left\| F\left[\hat{w}_j\right]\right\|_0 < s_1 \\ \left\|\Phi\left[\chi\right]\right\|_0 < s_2 \end{cases}$$

All tools

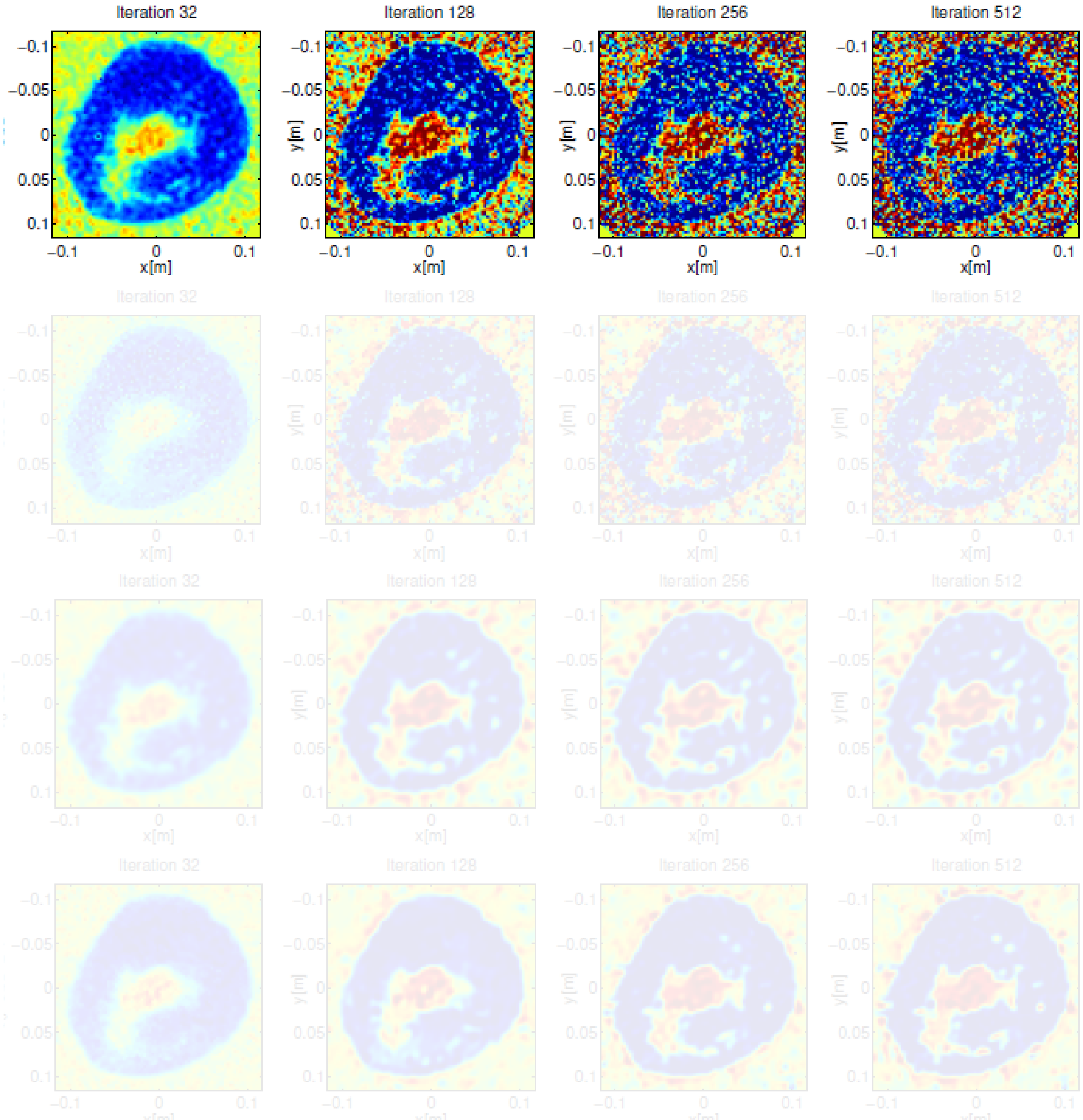

Frequency versus time domain

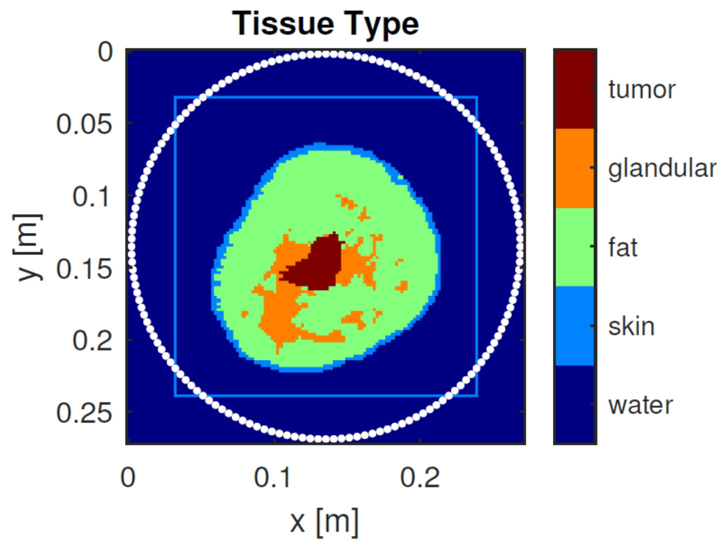

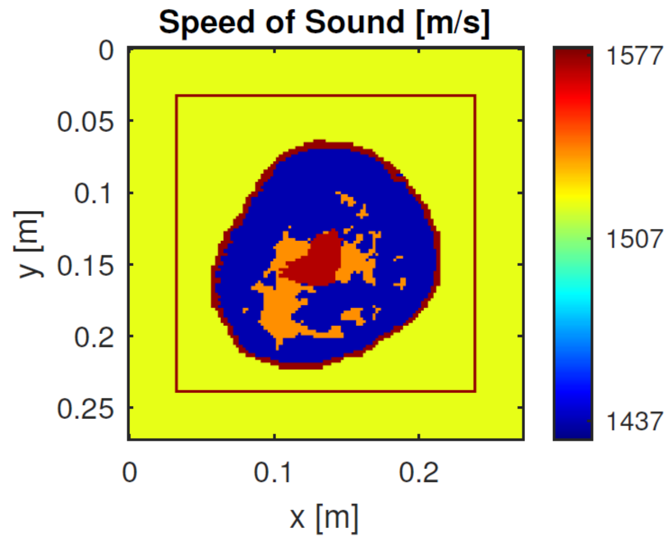

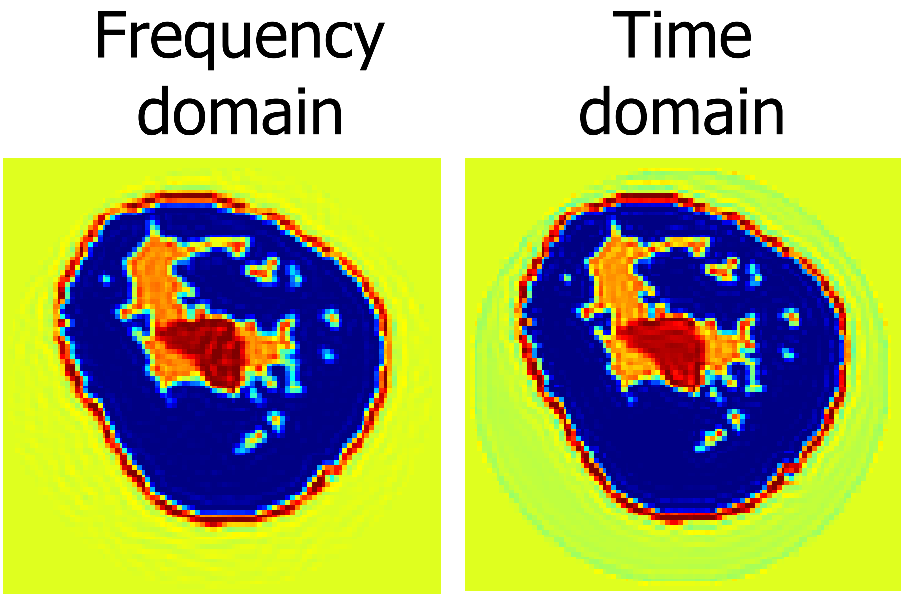

TUDelft

Multi-parameter Inversion

In reality, there is a contrasts in *compressibility and density*, besides attenuation.

True parameters

Single parameter

Multi parameter

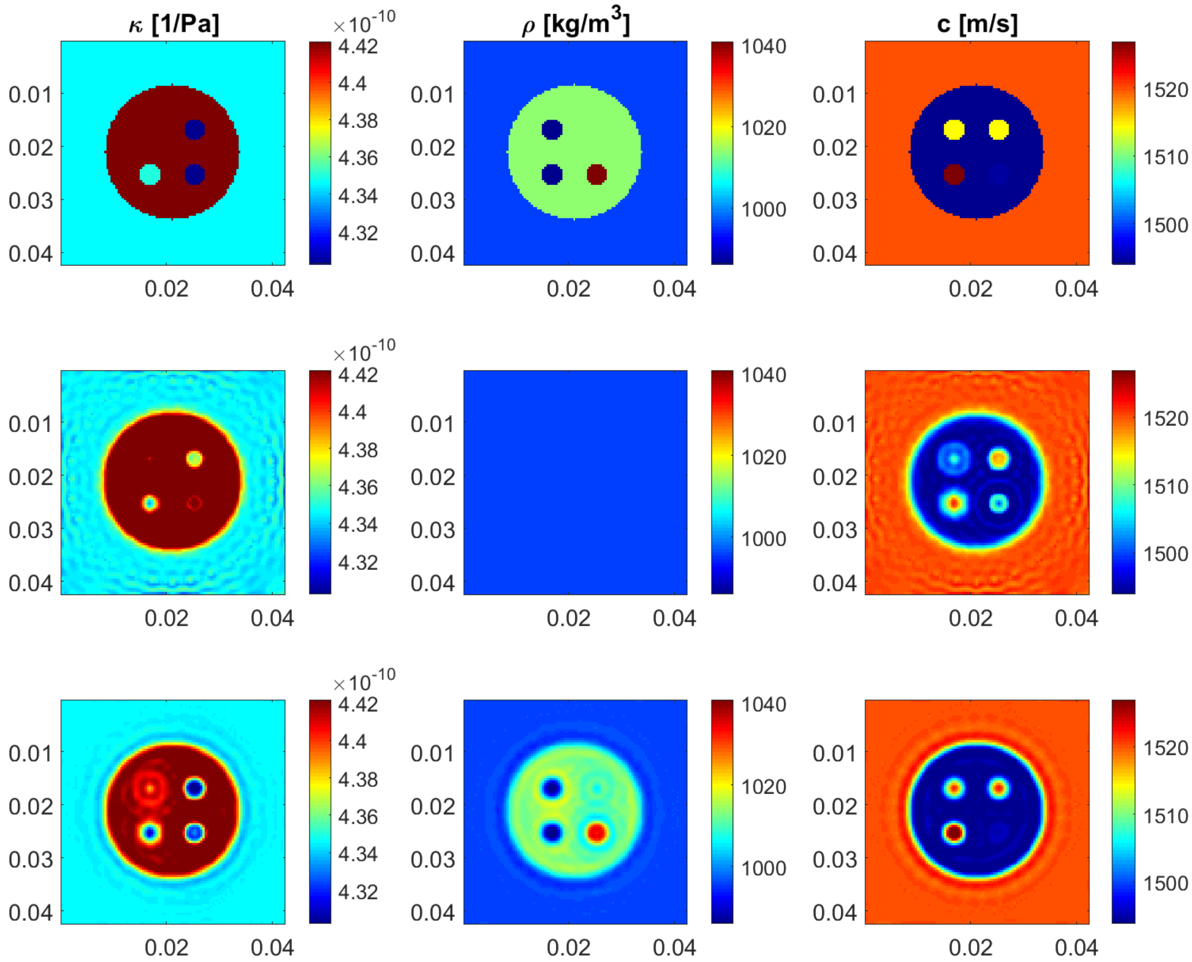

If needed, the velocity profile can be reconstructed from the pressure field!

U. Taskin et al, "Redatuming of 2-D Breast Ultrasound," IEEE Trans Ultrason Ferroelectr Freq Control 67(1)
U. Taskin et al, "Multi-parameter inversion with the aid of particle velocity field reconstruction," JASA 47(6)

TU Delft

Seismic Full Waveform Invention

Diving waves

original

reconstructed

Sound speed

Density

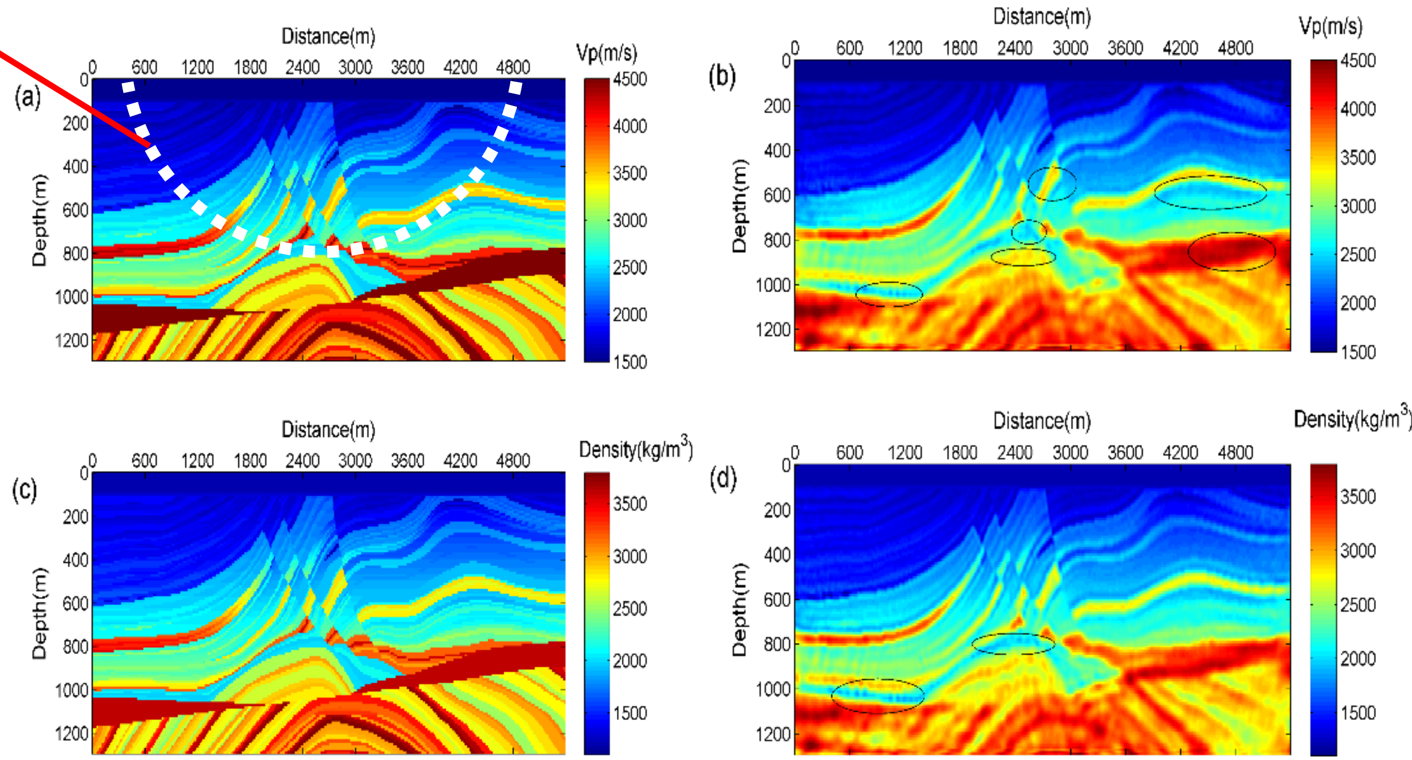

Zhong and Liu, "Time-domain acoustic full-waveform inversion based on dual sensor acquisition system," Journal of Seismic exploration (2019)

TU Delft

Transcranial Ultrasound

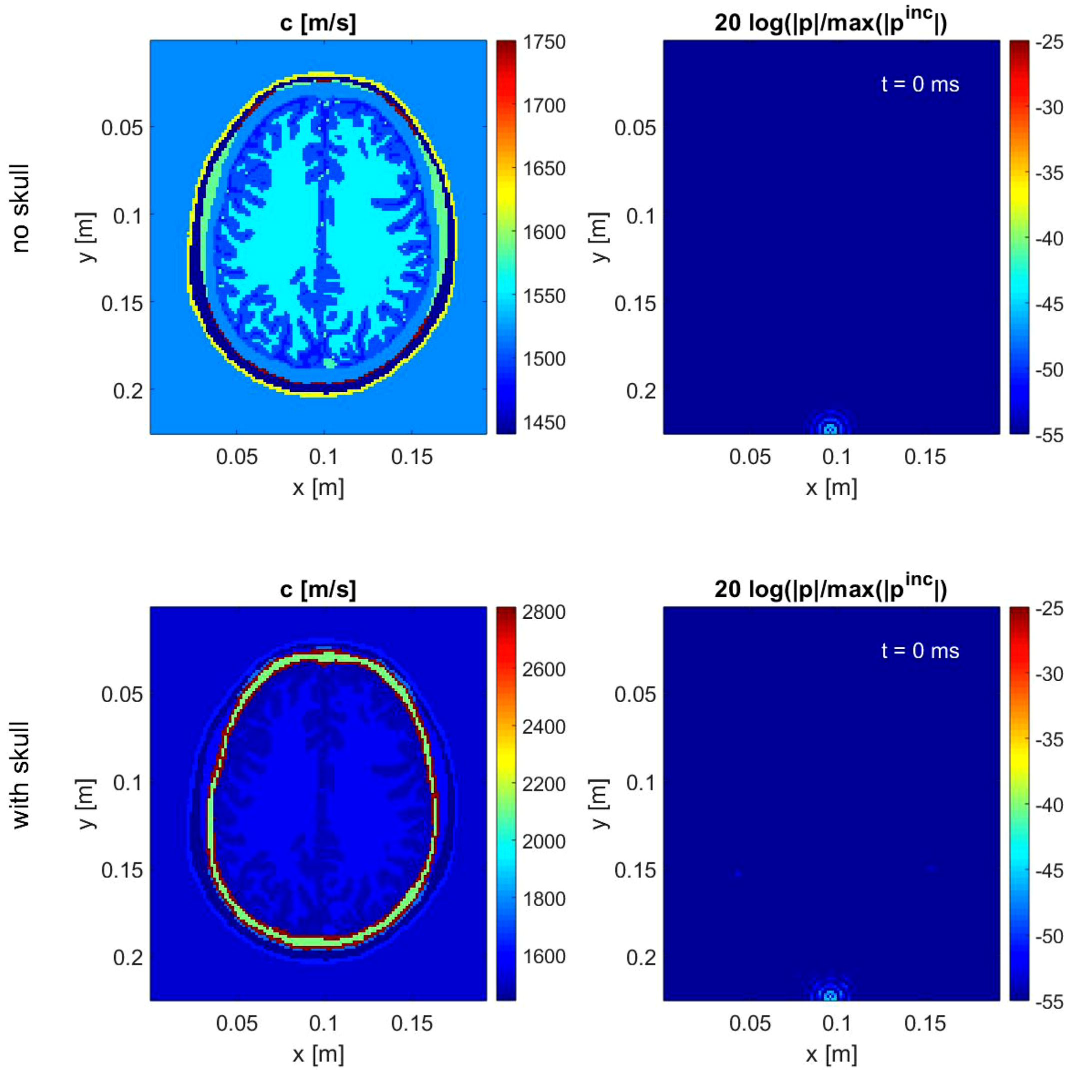

TU Delft

Transcranial Ultrasound

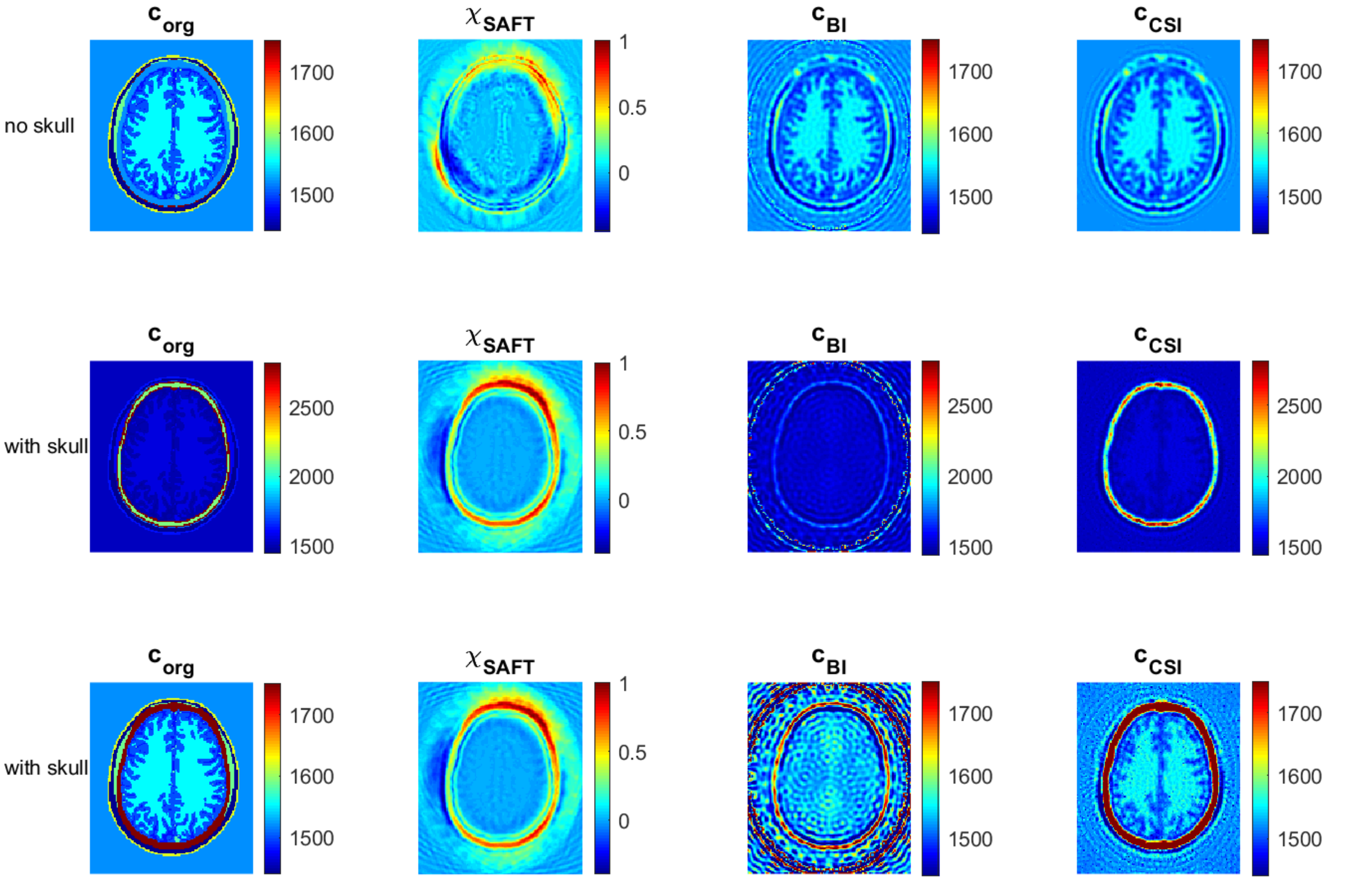

Imaging other body parts

- State of the art: 3-D FWI of breasts and other body parts as well the earth.

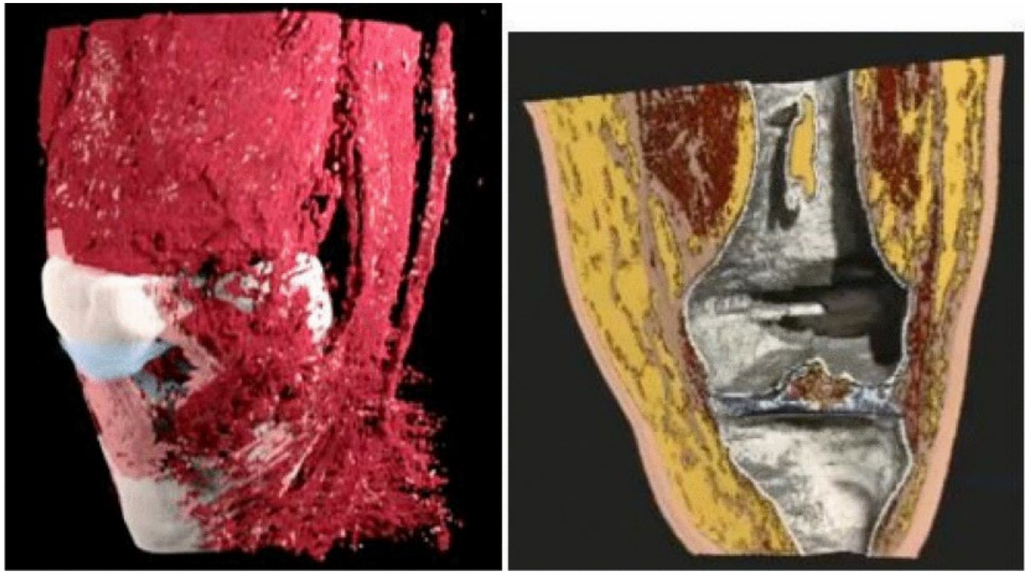

3D rendering of the SOS reconstruction of the human knee.

Wiskin, *et al.* "Full wave 3D inverse scattering transmission ultrasound tomography in the presence of high contrast," *Sci Rep* **10**, 20166 (2020)

Whole body imaging

- Anatomical correlation of pig abdomen

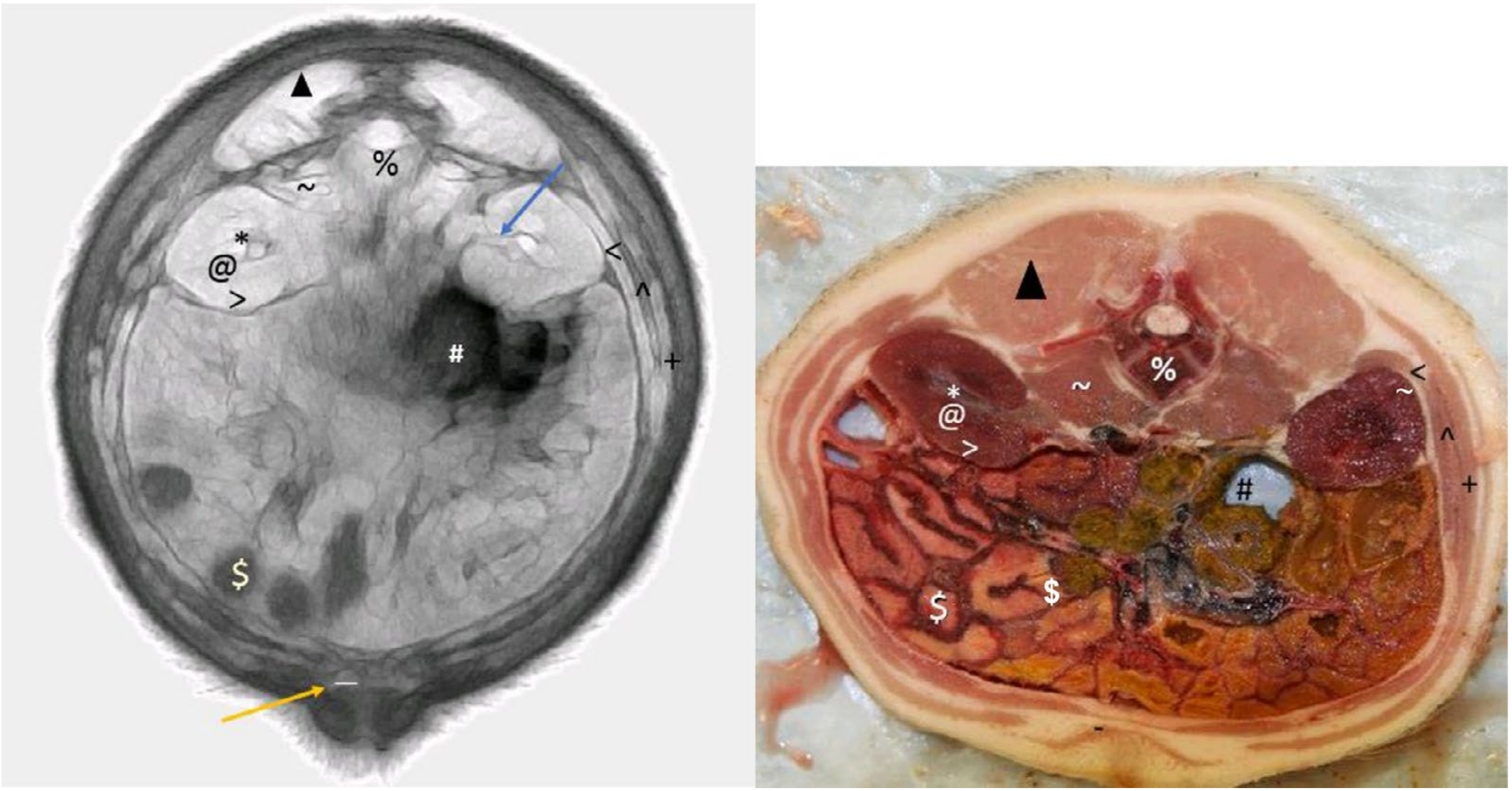

Wiskin et al., "Whole-Body Imaging Using Low Frequency Transmission Ultrasound, Academic Radiology (2023)

Machine learning for tissue classification

- QT Ultrasound
  - Based on 13 breasts
  - Tissue parameters only (?)

- Problems will occur to apply method to different systems

- Delphinus:
  Tissue parameters and Texture.

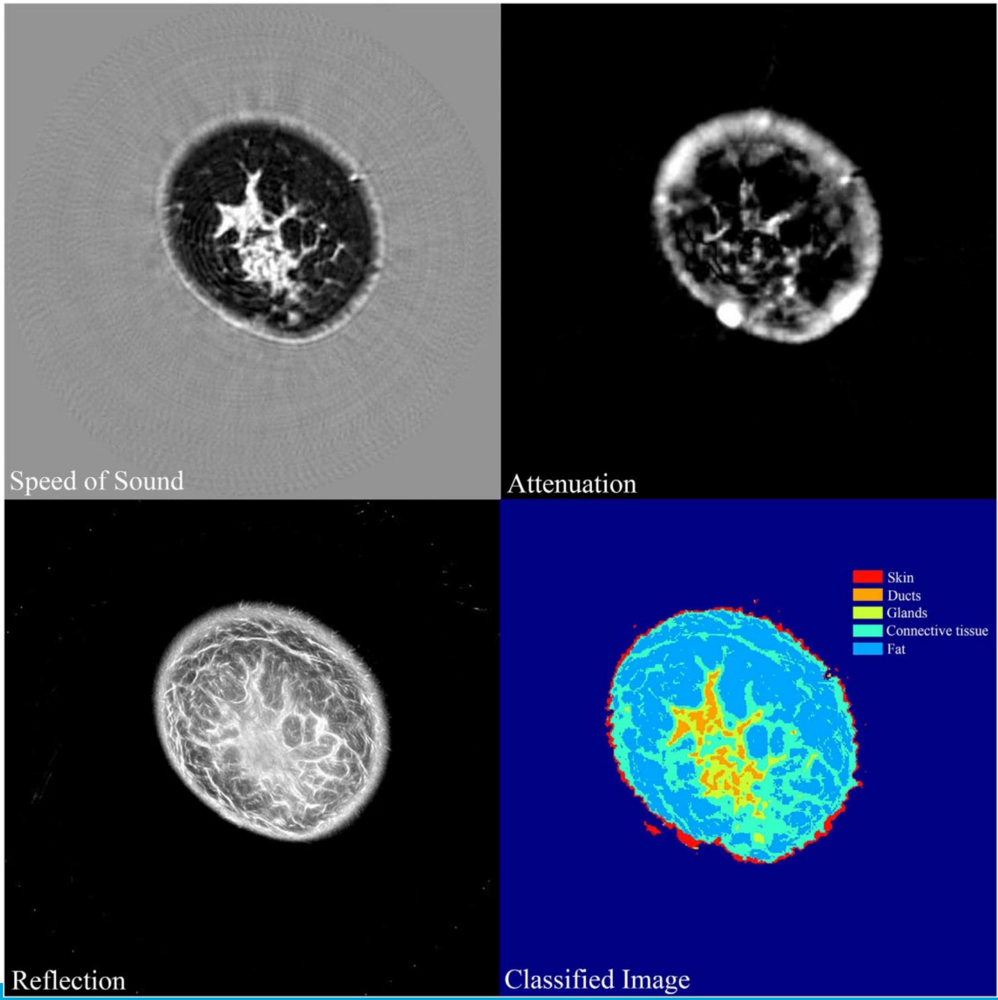

B. Malik, et al. "Objective breast tissue image classification using Quantitative Transmission ultrasound tomography," Scientific Reports, 2016

TU Delft

Machine learning for inversion

On synthetic data

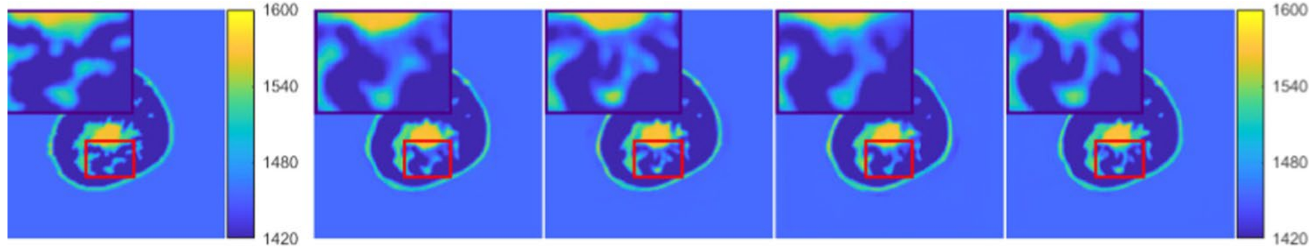

On real data

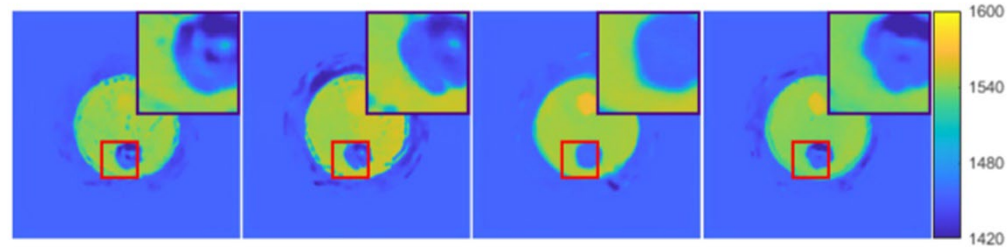

Zhao *et al* 2023, "Simulation-to-real generalization for deep-learning-based refraction-corrected ultrasound tomography image reconstruction," *Phys. Med. Biol.* **68** (2023)

Multi-parameter / joint inversion

Acoustics versus *Electromagnetics*,
both are waves …

… but with different:

- wavelengths & resolution,
- medium parameters !

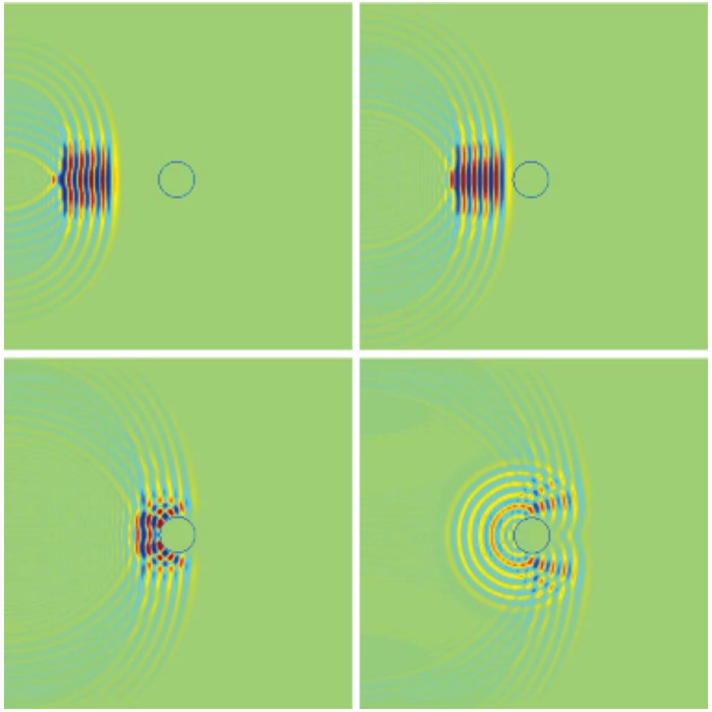

Multi-parameter / joint inversion

P wave velocity model

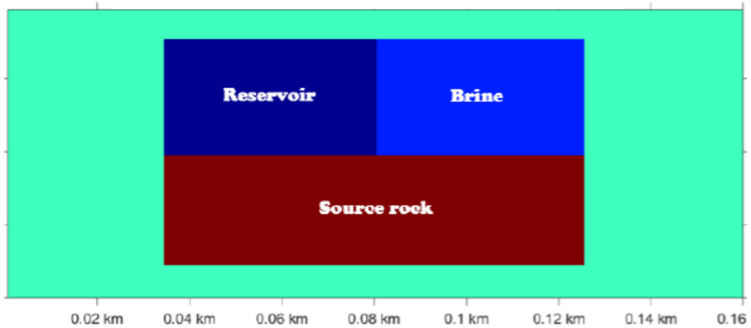

Acoustic Inversion

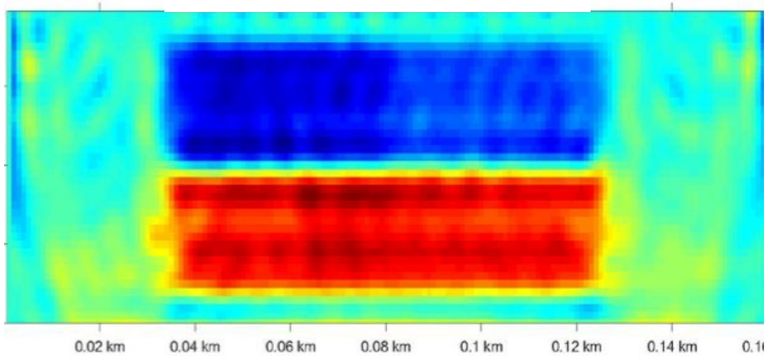

Resistivity model

EM Inversion

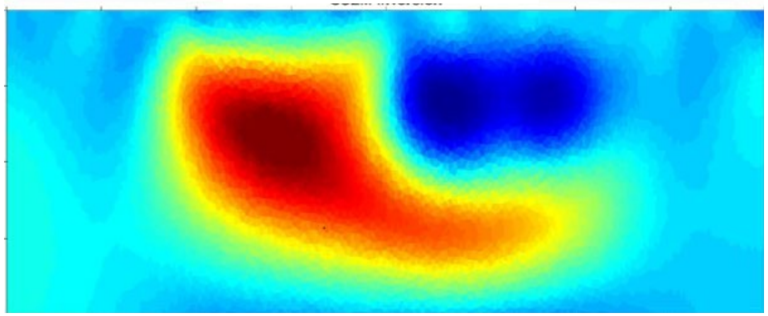

Multi-parameter / joint inversion

Can we

- *use one reconstruction to enhance the other in an iterative manner?*

Multi-physics / multi-parameter / joint inversion:

- simultaneous invert for multiple medium parameters,
- regularisation based on structural similarity.

acoustic

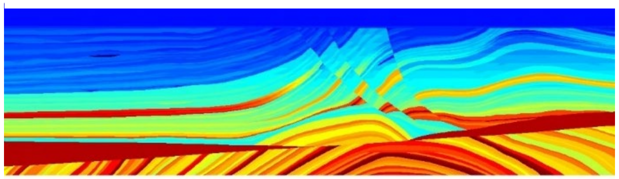

electromagnetic

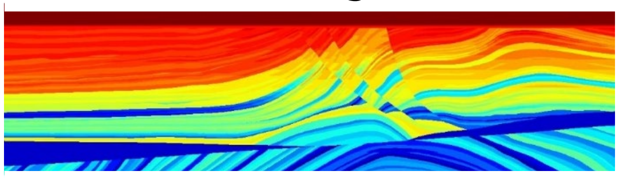

gravity

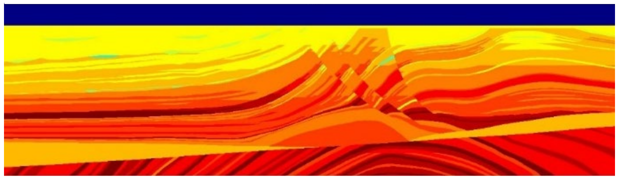

Multi-parameter / joint inversion

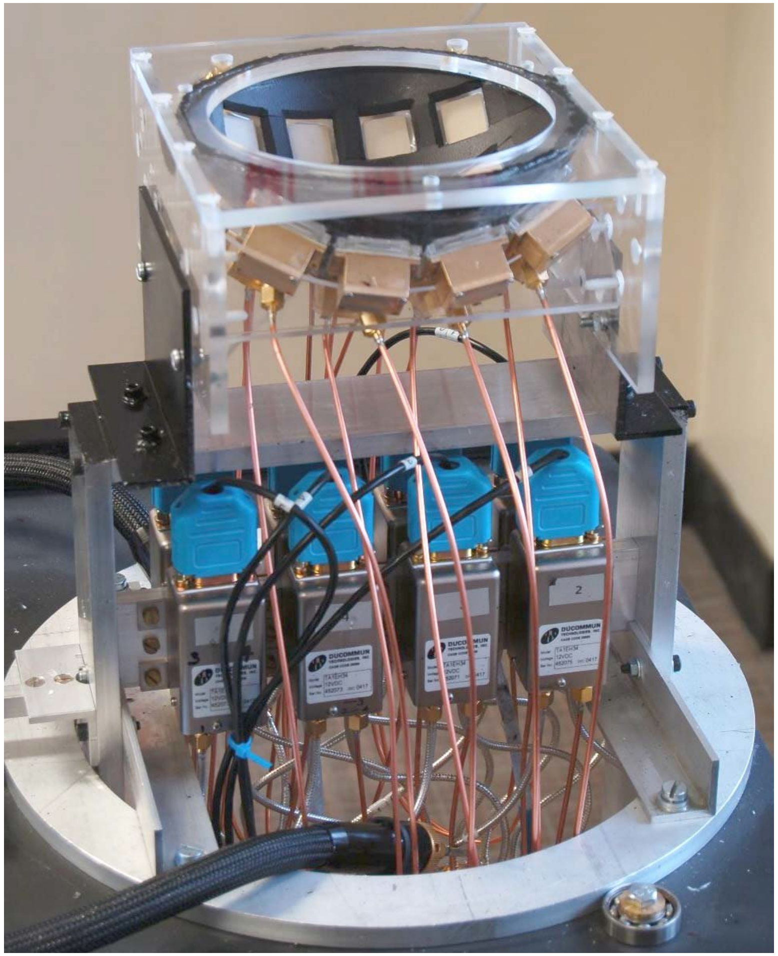

Klemm et al., "Experimental and clinical results of breast cancer detection using UWB microwave radar," 2008 IEEE Antennas and Propagation Society International Symposium, 2008.

Multi-parameter / joint inversion

Acoustic

$$\nabla^2 p - \frac{1}{c_{0;AC}^2}\partial_t^2 p = -S_{pr} - \underbrace{\chi_{AC}\partial_t^2 p}_{S_{cs}(\underline{r},t)} \quad \text{with } \chi_{AC} = \frac{1}{c_{0;AC}^2} - \frac{1}{c_{AC}^2(\underline{r})}$$

⇓ Fourier Transform

$$\nabla^2 \hat{p} + \frac{\omega^2}{c_{0;AC}^2}\hat{p} = -\hat{S}_{pr} + \chi_{AC}\omega^2 \hat{p}$$

⇓ Integral Equation

$$\hat{p} = \hat{p}^{inc} - \hat{G} *_{\underline{r}} \left[\chi_{AC}\omega^2 \hat{p}\right]$$

⇓ Forward / Inverse

Forward problem $\Leftarrow \hat{p}^{inc} = \hat{p} + \hat{G} *_{\underline{r}} \left[\chi_{AC}\omega^2 \hat{p}\right] \Leftrightarrow$ p^{inc}=Ap

Inverse problem $\Leftarrow \hat{p}^{sct} = -\hat{G} *_{\underline{r}} \left[\chi_{AC}\omega^2 \hat{p}^{inc}\right] \Leftrightarrow$ p^{sct}=A x

Electromagnetic TM

$$\nabla^2 \underline{E} - \frac{1}{c_{0;EM}^2}\partial_t^2 \underline{E} = -S_{pr} - \underbrace{\chi_{EM}\partial_t^2 \underline{E}}_{S_{cs}(\underline{r},t)} \quad \text{with } \chi_{EM} = \frac{1}{c_{0;EM}^2} - \frac{1}{c_{EM}^2(\underline{r})}$$

⇓ Fourier Transform

$$\nabla^2 \underline{\hat{E}} + \frac{\omega^2}{c_{0;EM}^2}\underline{\hat{E}} = \hat{S}_{pr} - \chi_{EM}\omega^2 \underline{\hat{E}} + \nabla\left[\nabla \bullet \underline{\hat{E}}\right]$$

⇓ Integral Equation

$$\underline{\hat{E}} = \underline{\hat{E}}^{inc} + \hat{G} *_{\underline{r}} \left(\chi_{EM}\omega^2 \underline{\hat{E}} - \nabla\left[\nabla \bullet \underline{\hat{E}}\right]\right)$$

⇓ Forward / Inverse

Forward problem $\Leftarrow \underline{\hat{E}}^{inc} = \underline{\hat{E}} + \hat{G} *_{\underline{r}} \left(\chi_{EM}\omega^2 \underline{\hat{E}} - \nabla\left[\nabla \bullet \underline{\hat{E}}\right]\right) \Leftrightarrow$ E^{inc}=BE

Inverse problem $\Leftarrow \underline{\hat{E}}^{sct}(\underline{r}) = -\hat{G} *_{\underline{r}} \left(\chi_{EM}\omega^2 \underline{\hat{E}}^{inc}\right) \Leftrightarrow$ E^{sct}=B x

TU Delft

Multi-parameter / joint inversion

$\lambda_{AC} = 15 \text{ mm} \ll \lambda_{EM} = 225 \text{ mm}$

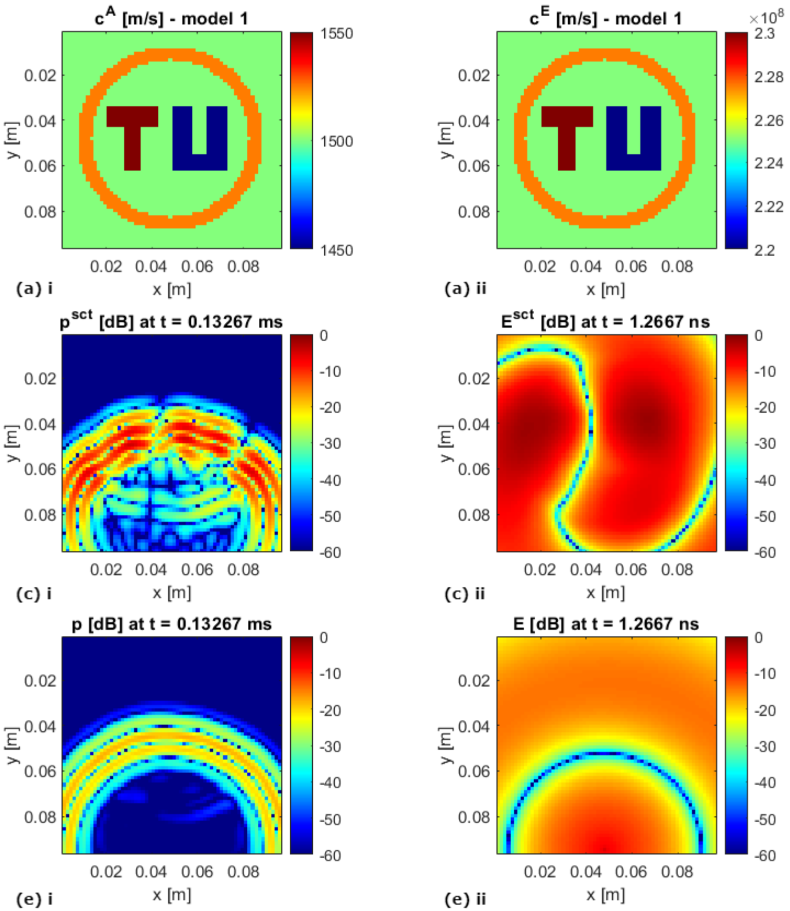

TU Delft

Joint inversion

$$\begin{pmatrix} r_{n;AC} \\ r_{n;EM} \end{pmatrix} = \begin{pmatrix} p^{sct}_{meas} \\ E^{sct}_{meas} \end{pmatrix} - \begin{pmatrix} G^{AC}\left[\chi_{n;AC}\right] \\ G^{EM}\left[\chi_{n;EM}\right] \end{pmatrix}$$

$$\begin{pmatrix} \chi_{n;AC} \\ \chi_{n;EM} \end{pmatrix} = \begin{pmatrix} \chi_{n-1;AC} \\ \chi_{n-1;EM} \end{pmatrix} + \begin{pmatrix} \alpha_{n;AC} d_{n;AC} \\ \alpha_{n;EM} d_{n;EM} \end{pmatrix}$$

$$\Leftrightarrow \quad Err_n = \frac{\left\| \begin{pmatrix} r_{n;AC} \\ r_{n;EM} \end{pmatrix} \right\|^2}{\left\| \begin{pmatrix} p^{sct}_{meas} \\ E^{sct}_{meas} \end{pmatrix} \right\|^2} + \beta \left\| \nabla \chi_{n;AC} - \nabla \chi_{n;EM} \right\|^2$$

Old

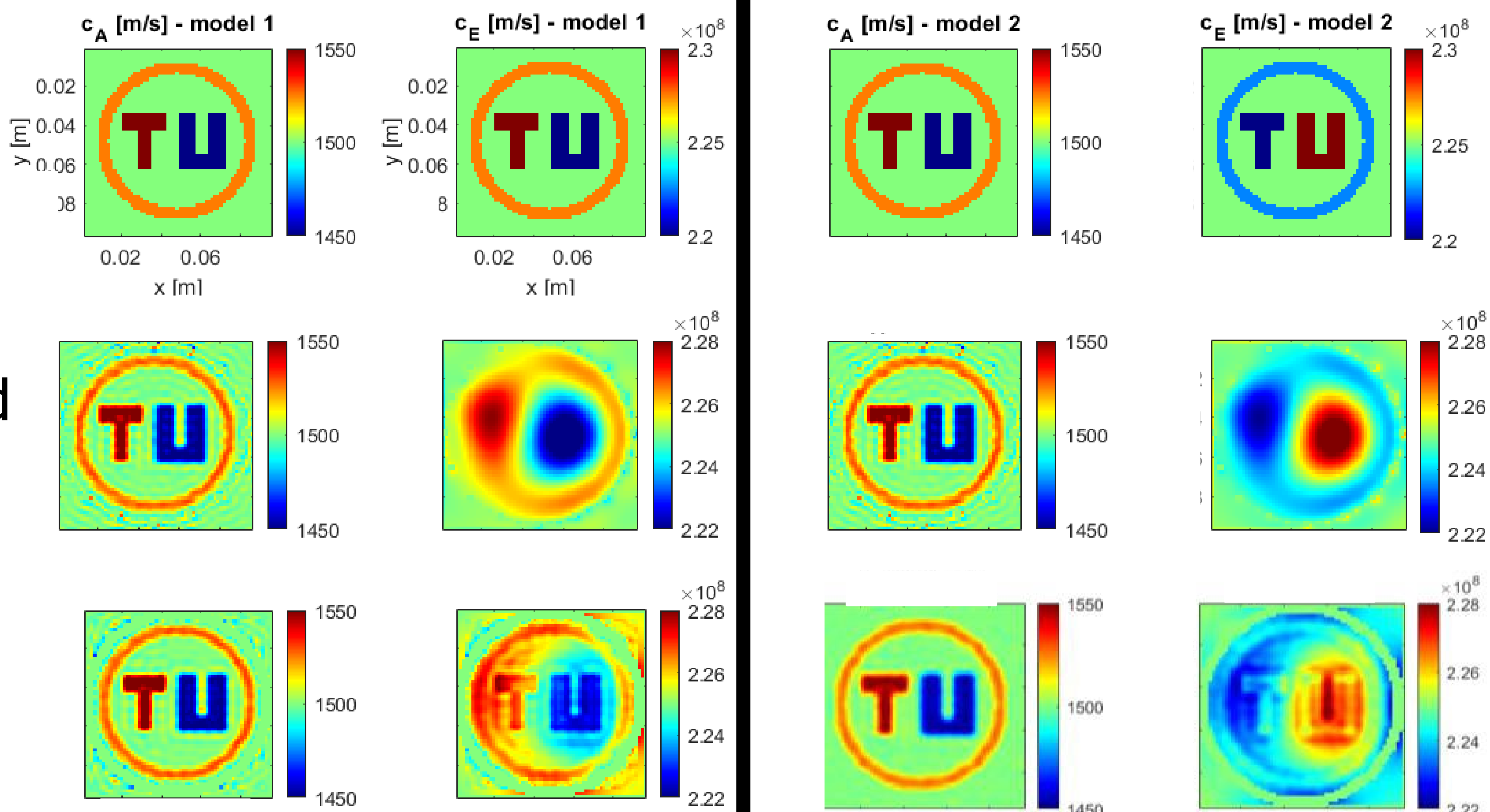

Low vs high frequency inversion – Breast US

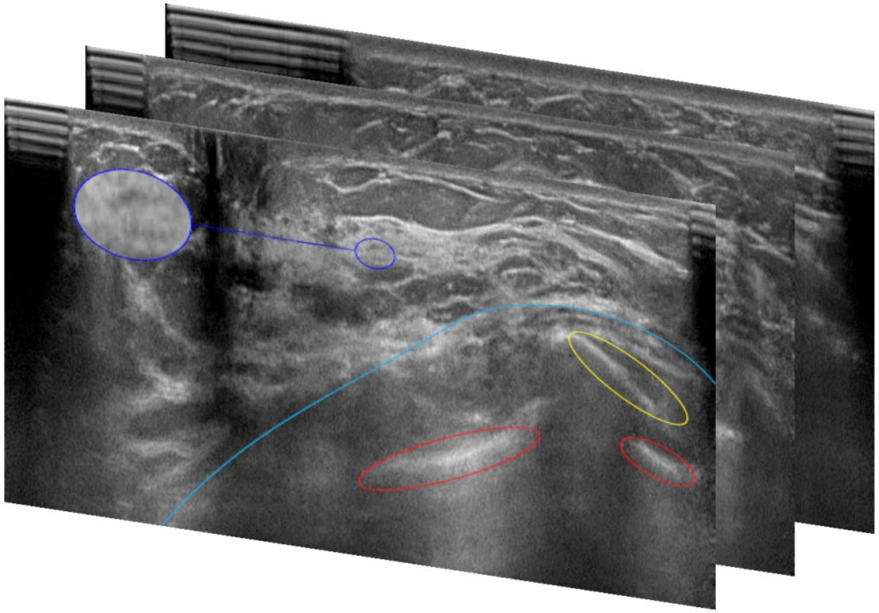

Radius = 80 mm
Δx = $\lambda/6$
$R\Delta\varphi$ = $\lambda/2$
N_f = 6

		F_0=0.5 MHz λ=3 mm	F_0=2 MHz λ=0.76 mm
N_{rec}	2-D	330	$1.3 \cdot 10^3$
	3-D	$17 \cdot 10^3$	$2.7 \cdot 10^5$
N_{src}	2-D	236	947
	3-D	475	$1.8 \cdot 10^3$
N_{unk}	2-D	$78 \cdot 10^3$	$1.2 \cdot 10^6$
	3-D	$8.2 \cdot 10^6$	$0.5 \cdot 10^9$
Mem	2-D	7 GB	455 GB
	3-D	1.4 TB	380 TB

Mem ≈ 4 fields x N_{unk} x N_{src} x N_f x 16

TU Delft

Discussion and conclusion

SAFT

- Echogenicity
- High frequency

Geometric / Ray based methods

- Speed of sound and attenuation
- High frequency
- Many src/rec combinations

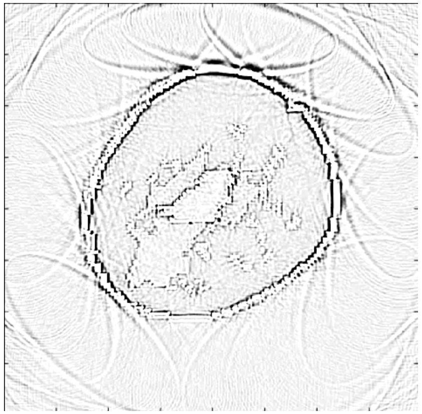

Born Inversion / Parabolic methods

- 2D - Neglects multiple scattering and phase shifts
- "Speed of sound & attenuation"
- Convergence

Full-Wave Form Inversion

- Taking advantage of multiple scattering and phase shifts
- Speed of sound & attenuation
- 3D - Computational heavy -> Low frequencies only

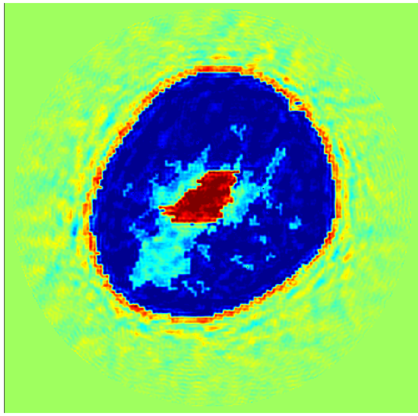

Machine learning

Multi-parameter / Joint Inversion

TUDelft

Day 5

TU Delft

History of Ultrasound

1942

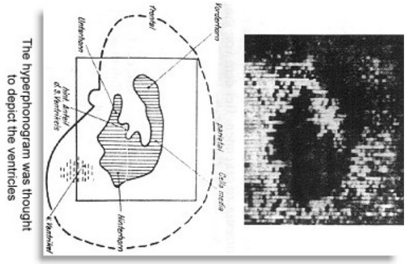

2020

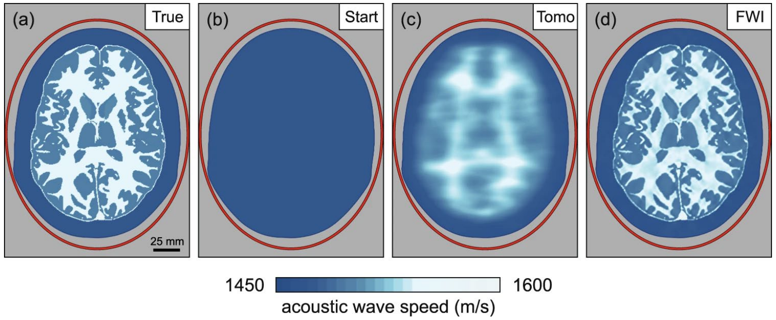

History of …

- Thales of Miletus 600 BC

- Thales is recognized for breaking from the use of mythology to explain the world and the universe, instead explaining natural objects and phenomena by offering naturalistic theories and hypotheses.

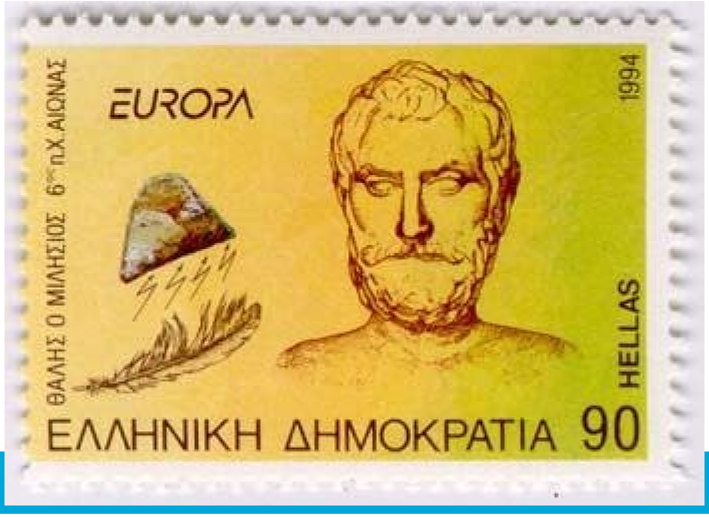

Part 1: History of ultrasound

1793 – Lazarro Spallanzani – Physiologist

Investigated the role of ultrasound for bats.

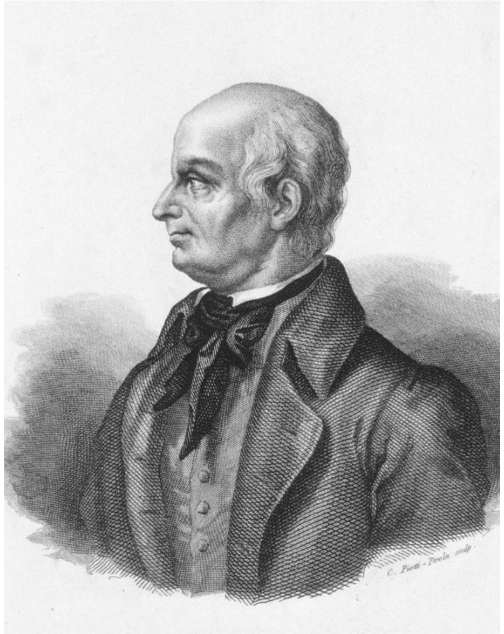

https://en.wikipedia.org/wiki/Lazzaro_Spallanzani

History of ultrasound

1880 – Pierre & Jacques Curie – physicists

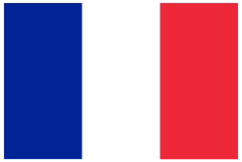

Discovery of the piezo-electric effect

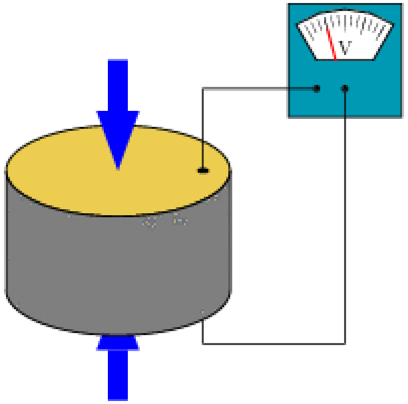

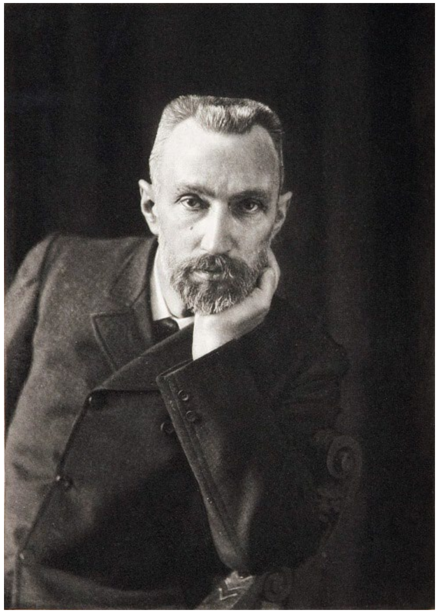

History of ultrasound

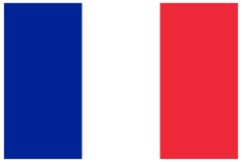

1916/1917 – Paul Langevin & Constantin Chilowsky - Physicists

- P. Langevin PhD degree with Pierre Curie (1902)
- Development of the transducer
  - To detect ice berg (Titanic, 1912)
  - WO I: April 23, 1916, sinking U-boat

History of ultrasound

1928 – S.Y. Sokolov – a Soviet physicist,

- ultrasound to find flaws in metal structures
- through transmission – shadow effects in the data

1944 – Floyd Firestone – United States

- patent for the *Reflectoscope*, first system in which the same transducer both generated the ultrasound waves, and also detected the reflected waves, in the time between transmitted wave pulses.

History of ultrasound

1942 – Karl Dussik – Neurologist & psychiatric
& Friederik Dussik – Physicist

- Imaging the brain

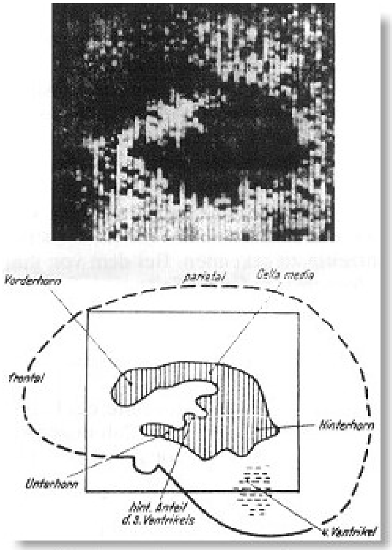

The hyperphonogram was thought to depict the ventricles

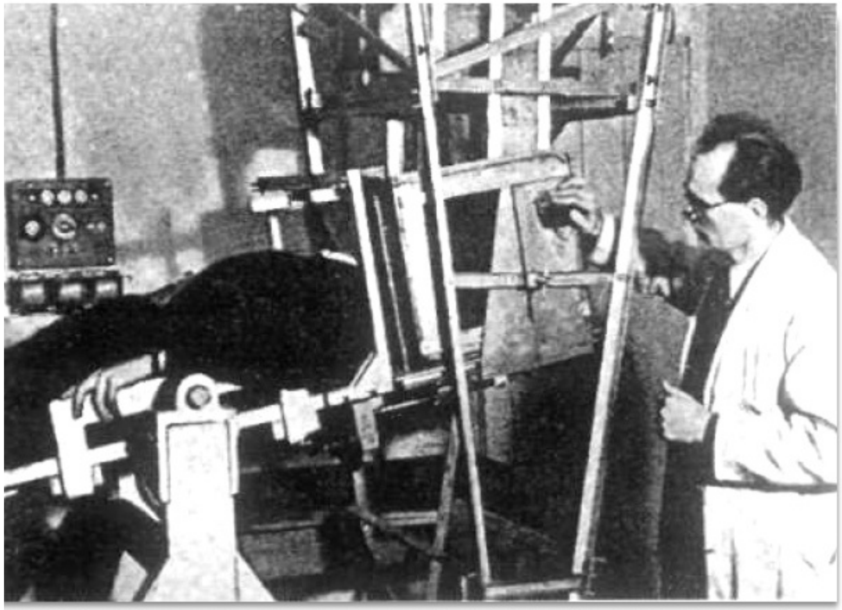

TU Delft

https://www.ob-ultrasound.net/dussikbio.html

History of ultrasound

1958 – Ian Donald – gynaecologist

- “Investigation of Abdominal Masses by Pulsed Ultrasound”, 7 June 1958, The Lancet

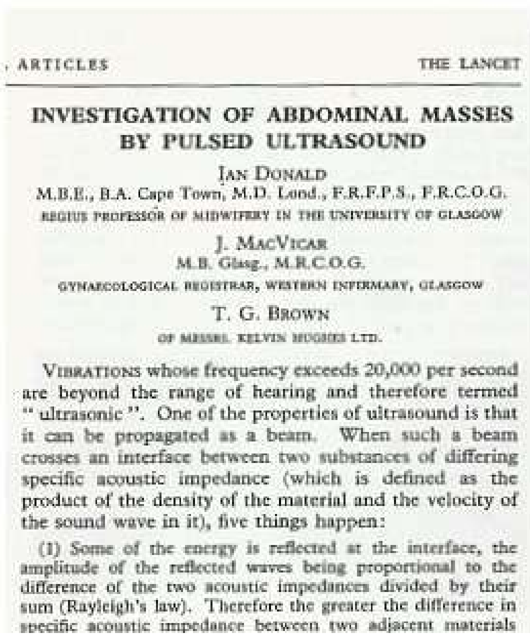

ARTICLES THE LANCET

INVESTIGATION OF ABDOMINAL MASSES BY PULSED ULTRASOUND

IAN DONALD
M.B.E., B.A. Cape Town, M.D. Lond., F.R.F.P.S., F.R.C.O.G.
REGIUS PROFESSOR OF MIDWIFERY IN THE UNIVERSITY OF GLASGOW

J. MACVICAR
M.B. Glasg., M.R.C.O.G.
GYNAECOLOGICAL REGISTRAR, WESTERN INFIRMARY, GLASGOW

T. G. BROWN
OF MESSRS. KELVIN HUGHES LTD.

VIBRATIONS whose frequency exceeds 20,000 per second are beyond the range of hearing and therefore termed “ ultrasonic ”. One of the properties of ultrasound is that it can be propagated as a beam. When such a beam crosses an interface between two substances of differing specific acoustic impedance (which is defined as the product of the density of the material and the velocity of the sound wave in it), five things happen:

(1) Some of the energy is reflected at the interface, the amplitude of the reflected waves being proportional to the difference of the two acoustic impedances divided by their sum (Rayleigh’s law). Therefore the greater the difference in specific acoustic impedance between two adjacent materials

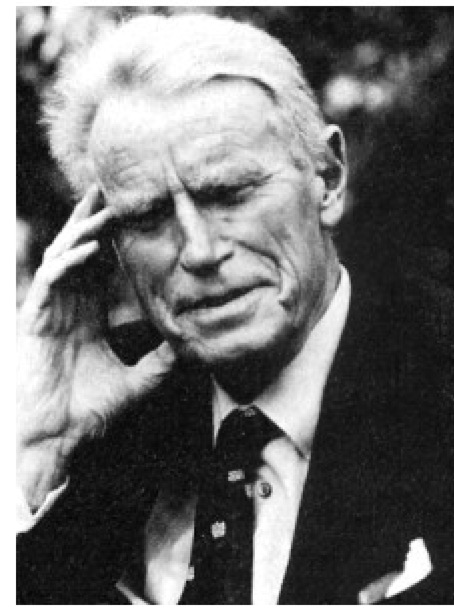

History of ultrasound

Fig. 2. Photograph of complete scanner table installed at Albany Medical Center. The bed is lowered to a horizontal position with the breast positioned through the hole.

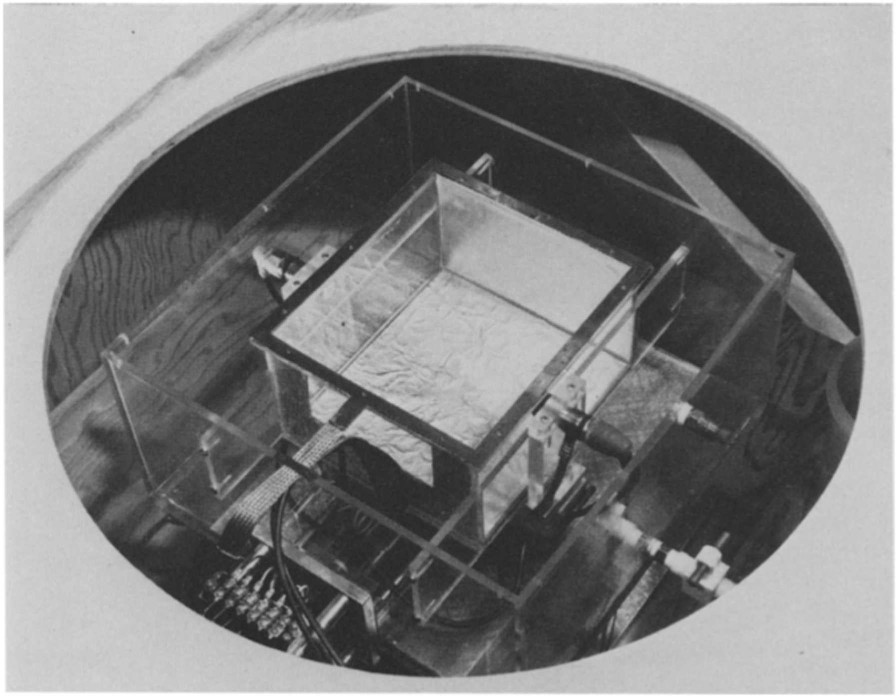

Fig. 3. Photograph of scanner mechanism. The entire tank rotates to obtain 100 projections. The breast is immersed in water in the inner box.

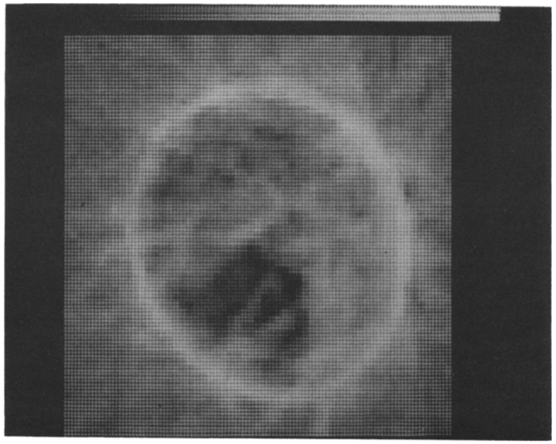

Fig. 6. Reconstruction for 24 year old asymptomatic person. Internal fibrous structure has velocity greater than that of water. Image size 10×10 cm.

Glover, "Computerized time-of-flight ultrasonic tomography for breast examination", Ultrasound Med. Biol. 3 (1977)

History of ultrasound

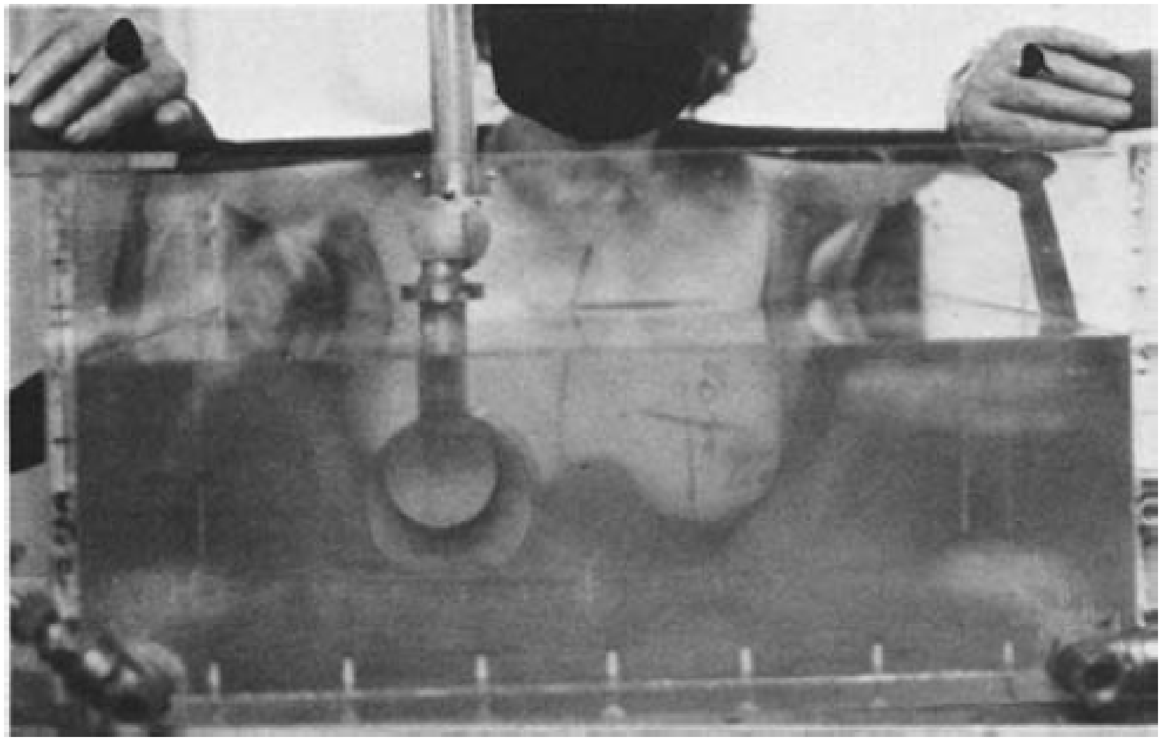

Fig. 2. Patient undergoing ultrasound mammographic examination. Direct water path coupling is used to avoid physical distortion of the breast.

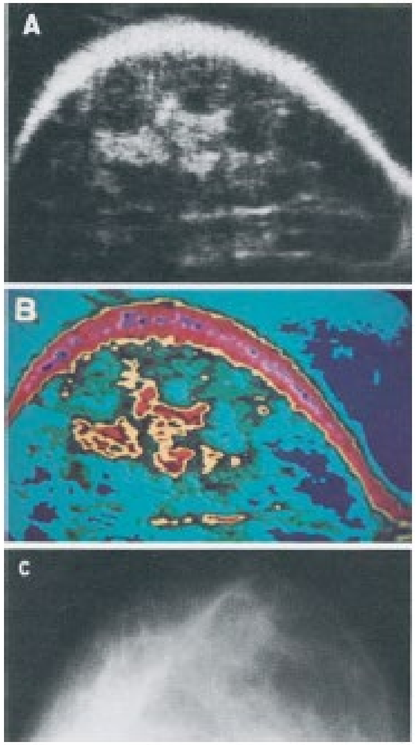

Fig. 5, A. Ultrasound mammogram of a 48-year-old woman. A loud echo-producing structure now lies in the center of the breast with an area of decreased reflectivity immediately anterior and posterior to it.

B. Color-coded isodensitometric printout of Figure 5, A.

C. Radiographic mammogram of Figure 5, A.

Baum, "Ultrasound Mammography", Ultrasound 1977

History of ultrasound

Fig. 3. (a) Pulse echo, (b) attenuation, and (c) speed-of-sound images obtained simultaneously in the right breast of a 55-year-old woman. The arrowheads indicate infiltrating ductal carcinoma (1510 m/sec). The lower bright spot represents the posterior portions of the subareolar tissues (1516 m/sec). The remainder of the breast plane is predominantly fatty tissue (1430 m/sec).

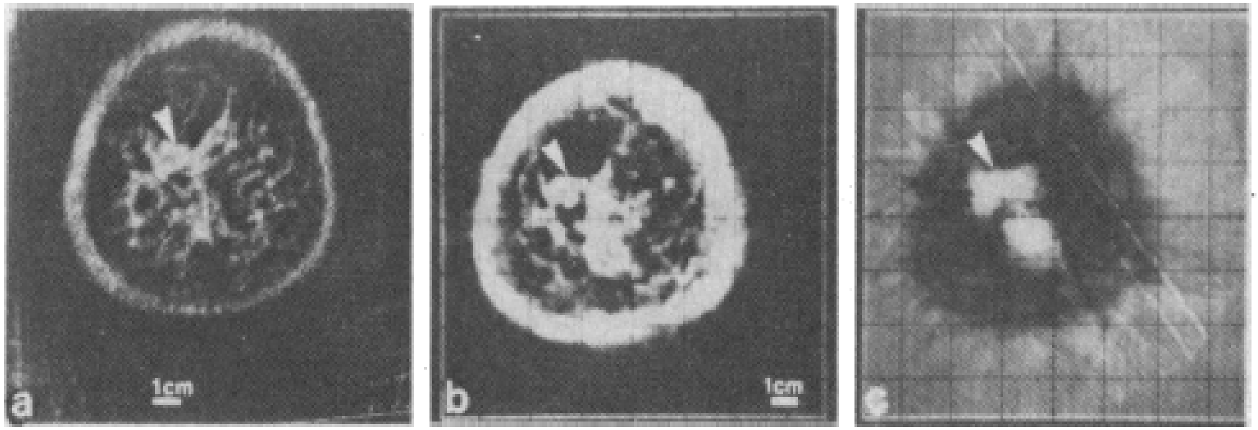

1142

Carson, Meyer, Scherzinger, Oughton, "Breast Imaging in Coronal Planes with Simultaneous Pulse Echo and Transmission Ultrasound", Science (1981)

History of ultrasound

1986 – Real-time orthogonal mode scanning of the heart.

J.E. Snyder, J. Kisslo, O.T. von Ramm

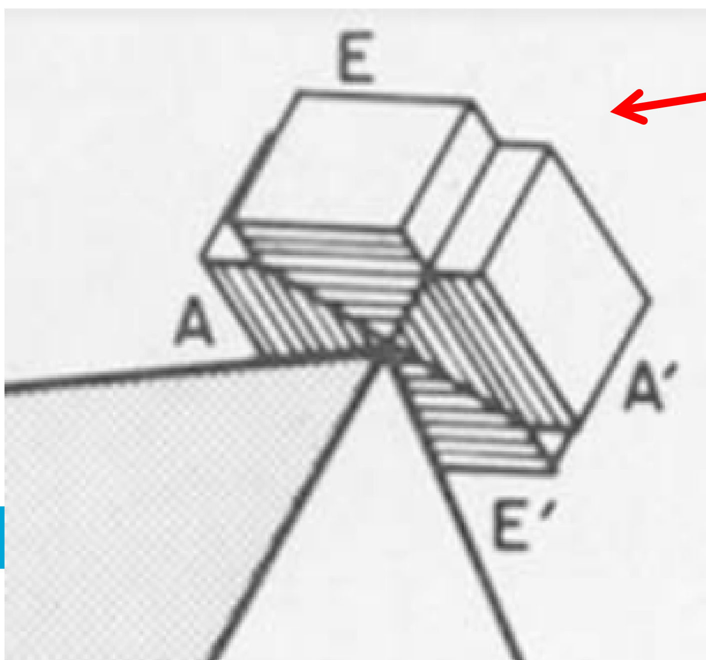

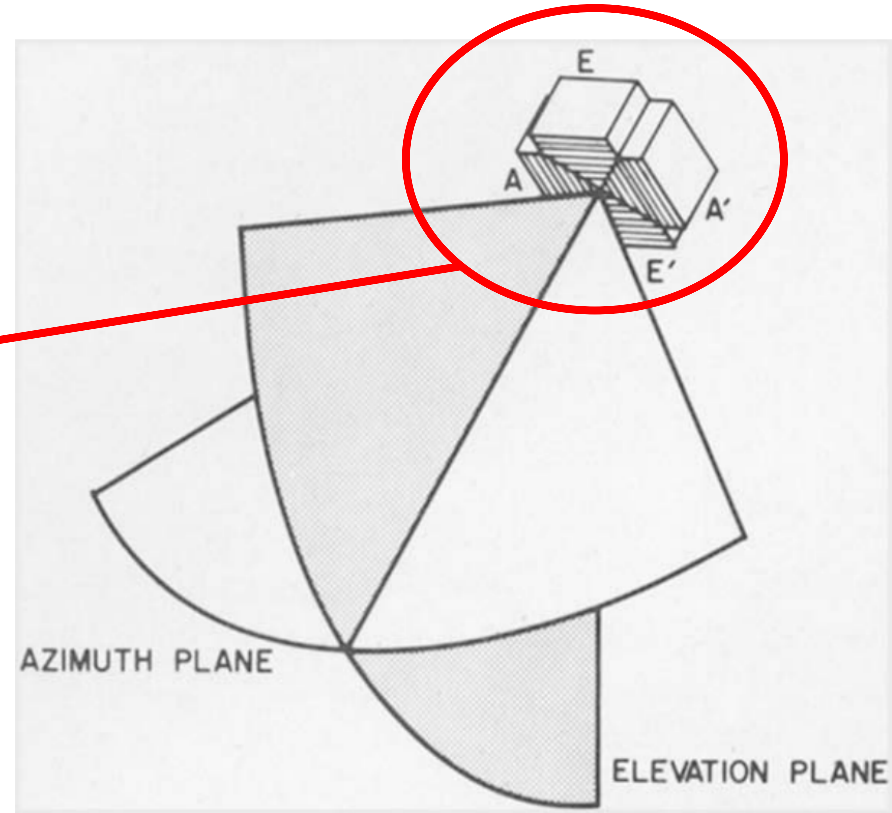

Figure 1. Schematic of the bow tie transducer and orientation of the orthogonal sector arcs. Four separate nearly triangular sections (A, A′, E and E′) comprise the O-mode array.

History of ultrasound

1991 – First hand held transducer for 3-D real-time ultrasound imaging

S.W. Smit, H.G. Pavy, O.T. von Raman

32 transmit channels
32 receive channels
17 x 17 elements

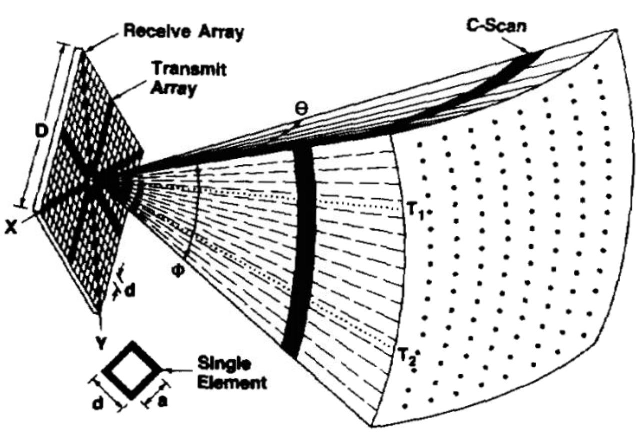

Fig. 1. Pyramidal scan format of 3-D ultrasound imaging system showing phased array transducer (front view), *C*-scan image plane and projection display points.

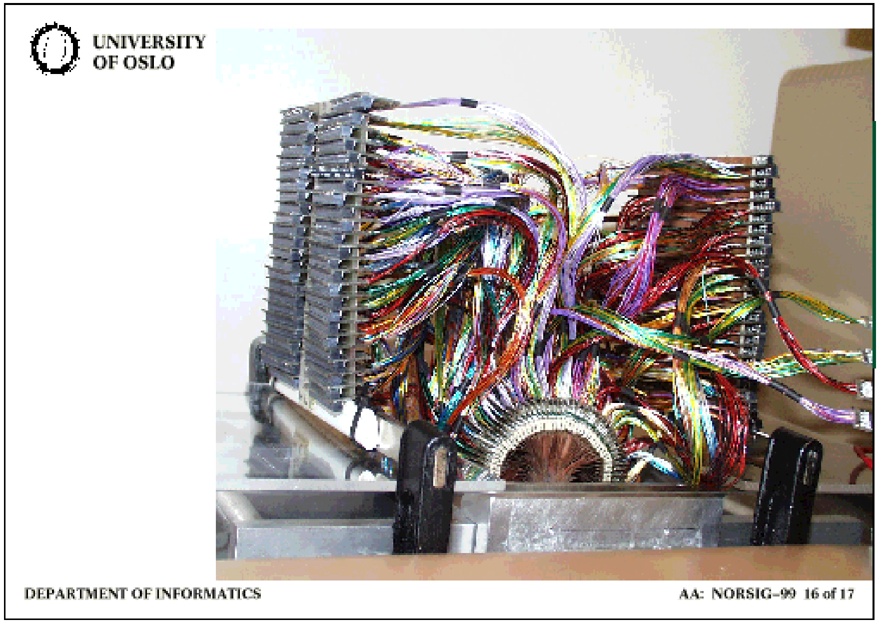

History of ultrasound

1991 – First hand held transducer for 3-D real-time ultrasound imaging

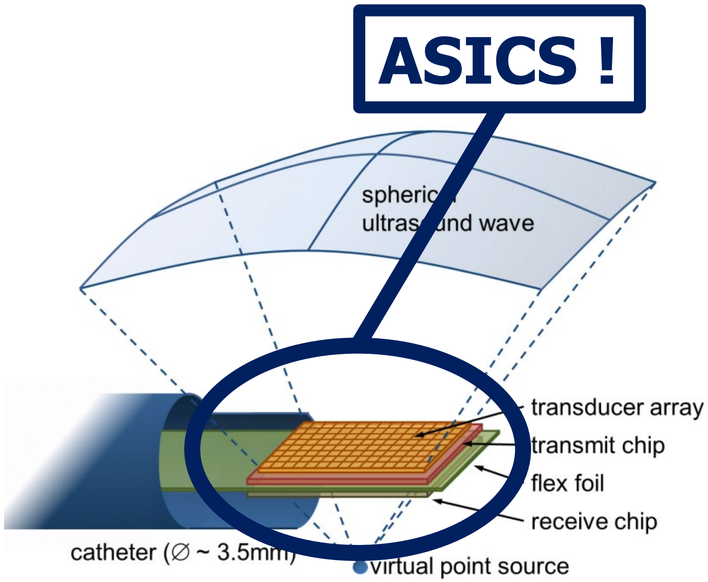

4.5 mm x 4.5 mm
120 µm x 120 µm

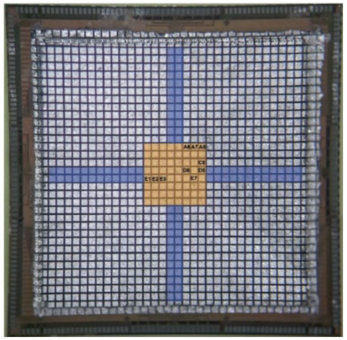

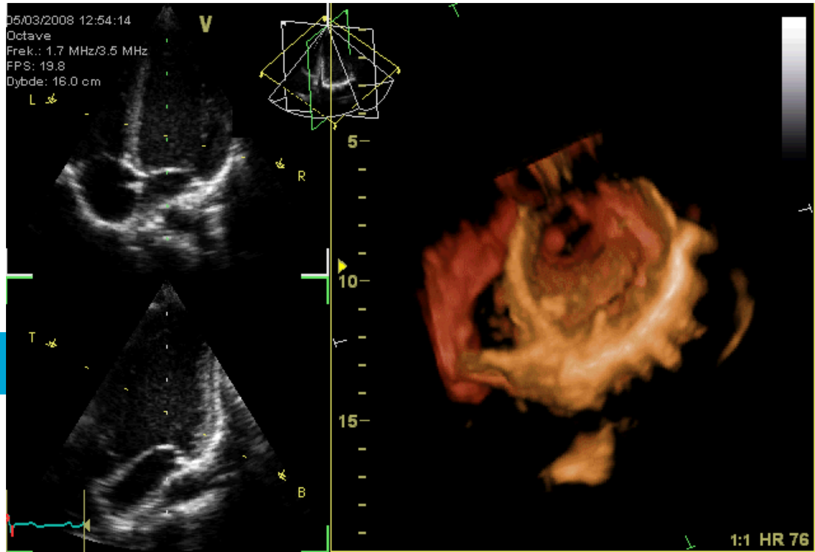

History of ultrasound

Brief history of seismic

- 1920s First analogue seismic measureme
- 1960s First computerized proces
- 1970s 2D multi-channel
- 1980s First 3D
- 2010 100,000
- 2017 system

The seismic community is one - two decades ahead of us!

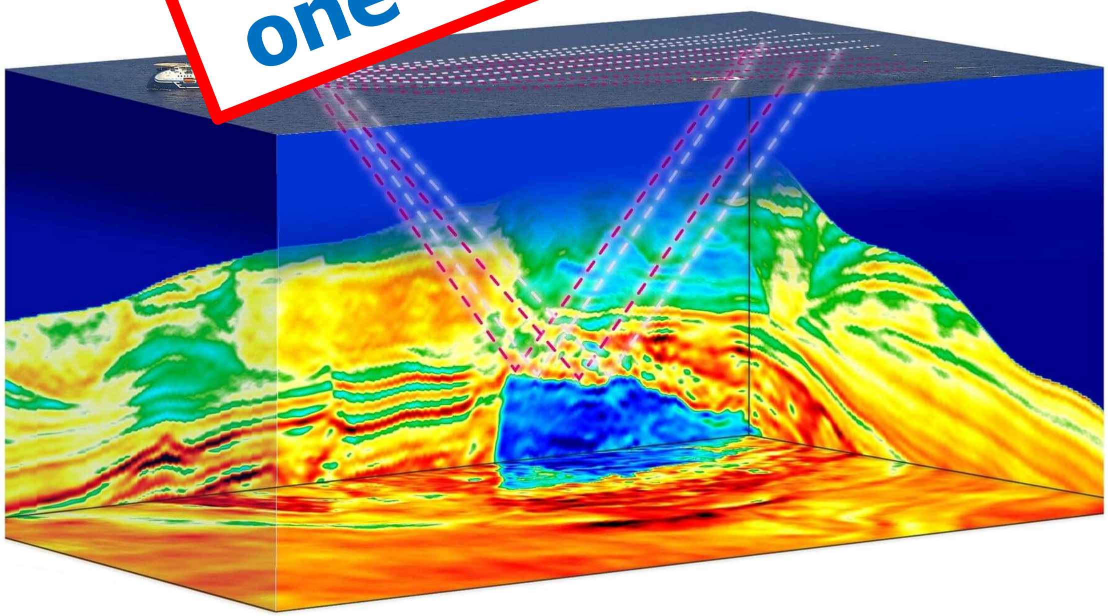

seismic survey in 1940's (wikipedia)

Medical vs seismic “survey”

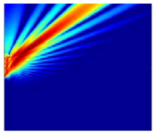

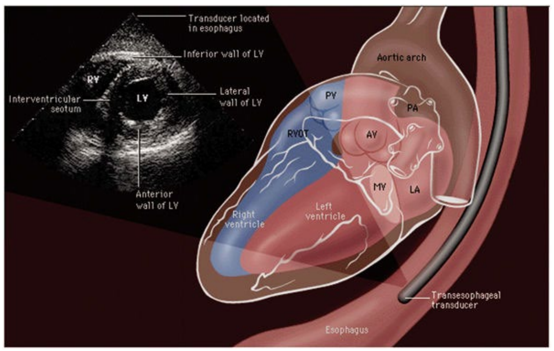

Medical	Seismic
F = 0.1 - 100 MHz	F = 0.1 - 1000 Hz
Real time	Days – weeks – months
Beam steering	Point sources / receivers
Geometric based	Wave based
1-128 channels	$>10^6$ channels
2D (3D)	3D
Price system 5-200 k€ Price scan 0.1-0.2 k€	? 5-700 k€ /km^2 (land)

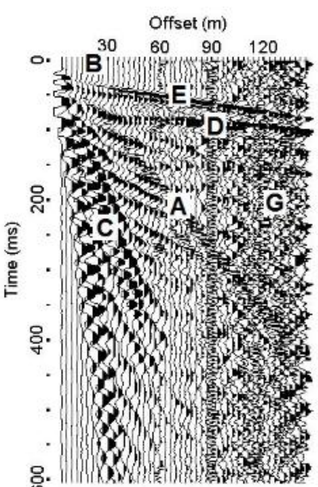

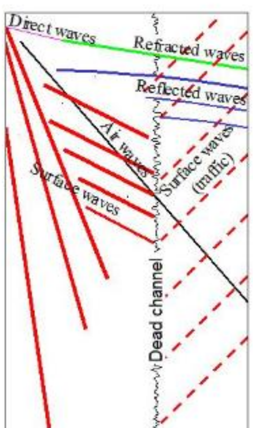

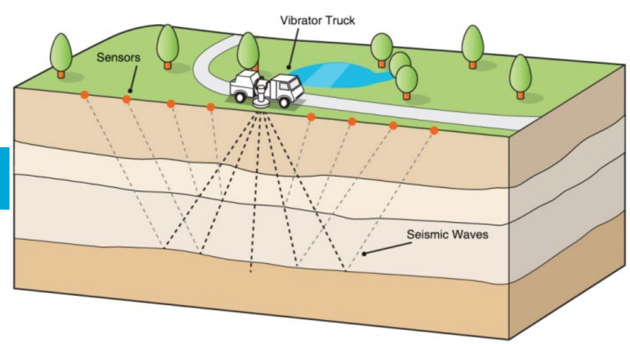

TU Delft